Optimal design of a CO_2 absorption unit and assessment of solvent degradation

PhD Thesis

Mid-Term Report

June 2011

Grégoire Léonard

Table of content

Figure Index

Table index

1 Introduction

1.1 Context of this work

Global climate change is a fact and the influence of human activity on this change through greenhouse gases' emission is widely recognized by the international scientific community. The largest emitted greenhouse gas is CO_2, and fossil fuel power plants are amongst the largest CO_2 emitters.

Regulatory frameworks, public opinions and scientific community all agree on the importance of acting now to reduce CO_2 emissions. The best way to do so is first to encourage energy savings and reduce energy losses. Then, the development of renewable energies has to be enhanced in order to become a large part of the future energy mix.

Many studies report that coal combustion will remain one of the largest power sources in the next decades (among others, see the World Energy Outlook, 2010). Three main solutions can contribute to the reduction of CO_2 emissions in coal power plants: continuous improvement of energy efficiency, which has already been performed to a large extent, biomass co-combustion and carbon capture and storage.

In this framework, Carbon Capture and Storage (CCS) technologies for power plants are a necessary technical development. They should perform the transition between our carbon-based society with its greenhouse gases emissions concerns and a society based on sustainable energy systems.

1.2 Post-combustion CO_2 capture

This work focuses on the post-combustion capture process. It is based on the reactive absorption of CO_2 with an amine solvent, most commonly an aqueous solution of 30 wt-% monoethanolamine (MEA, NH_2-CH_2-CH_2-OH, C_2H_7NO). The principle of this process is represented in figure 1.1.

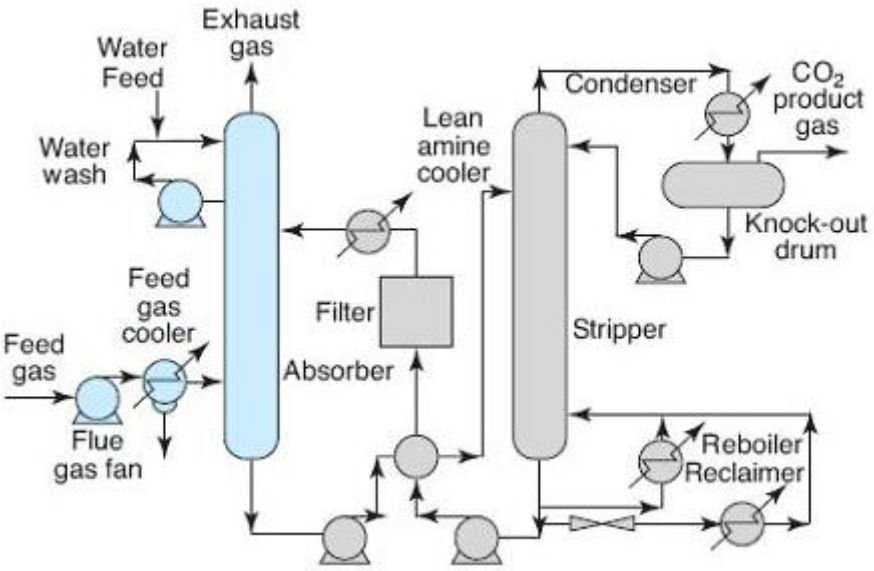

Figure 1.1: Flowsheet of the chemical absorption process (IPCC, 2005)

In the case of a coal power plant, the flue gas contains in volume approximately 14% CO_2, 6% O_2, 12% H_2O and 68% N_2. Some impurities (NOx, SOx, HCl, …) are still present in the flue gas, so that different gas purification steps are necessary, like FGD (flue gas desulfurization), SCR (selective catalytic reduction), and a wet pre-scrubbing treatment to remove the remaining SO_2 and achieve the desired temperature. After purification, the flue gas enters the absorption column (also named "absorber"). Carbon dioxide is absorbed with a chemical solvent at temperatures varying between 40 and 60°C depending on the solvent (55°C in the case of MEA). The main reactions taking place during the absorption are listed in table 1.1 for the MEA case.

Table 1.1: Chemical reactions of CO_2 absorption with MEA

$2\ H_2O \leftrightarrow H_3O^+ + OH^-$
$C_2H_7NO + H_3O^+ \leftrightarrow C_2H_8NO^+ + H_2O$
$CO_2 + 2\ H_2O \leftrightarrow H_3O^+ + HCO_3^-$
$HCO_3^- + H_2O \leftrightarrow H_3O^+ + CO_3^{2-}$
$C_2H_7NO + HCO_3^- \leftrightarrow C_3H_6NO_3^- + H_2O$

After CO_2 absorption, the treated flue gas usually flows through a water-wash section and a demister in which the entrained solvent droplets are separated from the gas. The CO_2-loaded solvent (also referred to as "rich solvent") is pumped to a regeneration column (also named "stripper") via an heat-exchanger where the rich solvent is pre-heated.

In the stripper, the solvent is regenerated at temperatures varying between 100 and 140°C (120°C in the case of MEA). The purpose of the reboiler at the stripper bottom is to supply heat for the solvent regeneration. At this temperature, the absorption reaction is counter-balanced by the desorption reaction, so that CO_2 is released from the solvent. The regenerated solvent ("lean solvent") is fed back to the absorber via the rich-lean heat exchanger where it gives its energy to pre-heat the rich solvent. A further heat exchanger cools the regenerated solvent down to the right absorber entrance temperature.

The gaseous CO_2 stream at the exit of the desorption column contains some water that is removed in the condenser, so that the final product may reach a CO_2-purity of 99% by volume. The objective that is generally pursued in post-combustion processes is the removal of 90% of the CO_2 present in the power plant flue gas stream.

2 Objectives

Based on a master thesis written in 2009, this PhD thesis in the field of chemical engineering has been launched at the University of Liège in an industrial partnership with the company Laborelec, part of the GDF SUEZ group.

The first sub-topics of this PhD thesis is the simulation and the optimization of the CO_2 post-combustion capture process with amines. The Aspen Plus® software (Advanced System for Process Engineering) has been chosen as a performing simulation tool to simulate the CO_2 capture process. Once the model is built, the first goal is to identify process parameters that have the largest influence on the energy requirement of the CO_2 capture, to study their influence on the process, and to optimize them. This has already been performed based on a sensitivity analysis for which results are presented in chapter 3. The second goal of the simulation part is to dispose of a precise model that describes a pilot CO_2 capture installation for which Laborelec has been associated to the development. This model – the same that has undergone the optimization procedure – should be validated using experimental data from the pilot installation as soon as those will be available.

The second sub-topic of the thesis concerns the degradation of amine solvents used for CO_2 capture. It is detailed in chapter 4. Since amine degradation is due to chemical reactions with slow kinetics, a degradation test rig has been constructed at the University of Liège for the experimental study of accelerated degradation under high pressure and high temperature conditions. This equipment allows the study of amine degradation in batch mode as well as in semi-batch mode, by which a gas continuously flows through the solvent solution. A particular interest will be devoted to the degradation of MEA solutions, since MEA is the most widely used amine for CO_2 capture. However, some alternative solvents should also be tested. The influence of different parameters (temperature, pressure, gas composition and mass flow) on solvent degradation will be identified and quantified. Furthermore, since corrosion and degradation inhibitors are commonly used in industrial processes, their impact will be studied as well.

The innovative contribution of this thesis is the development of a link between those sub-topics. Indeed, degradation as well as process modeling are performed in different research groups. However, the construction of a simulation model including process efficiency criteria as well as degradation-related influence factors has not been performed yet. Using this model, a multi-objective optimization will be conducted in order to propose optimal operating conditions for the CO_2 capture process regarding energy efficiency as well as degradation and environmental performance. This model should give a better understanding of the complex relations between degradation and process efficiency. It will furthermore help to find and optimum between economical concerns (process efficiency) and environmental ones (emission of degradation products).

3 Modeling

The first sub-topic of the PhD thesis is the modeling of the post-combustion CO_2 capture with amine solvents. The first objective of this simulation work is to highlight the key process parameters and their influence on the process efficiency through a sensitivity analysis and without running long and costly experiments. Moreover, the influence of some process technical improvements can be studied at low cost expense thanks to simulation. Then, the second objective is to validate a CO_2 capture model developed to simulate a particular pilot plant for which the industrial partner Laborelec has been associated to the development

The models developed in this work simulate a steady state carbon capture process with monoethanolamine (MEA) as absorption solvent. The flue gas treated comes from a typical coal power plant and corresponds to one train of operation of the pilot developed in collaboration with Laborelec (2500Nm^3/h with flue gas volume composition of 14% CO_2, 6% O_2, 12% H_2O and 68% N_2). The energy requirement at the stripper reboiler is adjusted in order to insure a capture rate of 90% (which corresponds to a capture rate of about 1 ton CO_2/h).

This chapter will first shortly consider the equilibrium model available at the beginning of this PhD thesis and then describe the rate-based model that has been developed to take into account the kinetics and mass transfer limitations in the columns. Simulation results are presented in section 3.3, considering first a sensitivity study of the main process parameters on the process energy requirement and second the influence of some process flowsheet modifications. Finally, some perspectives are evocated at the end of this chapter. The validation process is not described in this work since it has still to be performed as soon as experimental results will be available.

3.1 Equilibrium model

The first model that has been developed at the University of Liège is an equilibrium model based on a previous work made at the University of Delft in collaboration with the TNO institute (Abu Zahra, 2009). In this model, the absorber and the stripper are modeled using the assumption that each theoretical column stage is at a state of thermodynamic and chemical equilibrium. It means that the vapor leaving each theoretical stage of the column is in a perfect equilibrium state with the liquid leaving this same stage. However, equilibrium is never reached in the reality since limitations occur in the reaction kinetics and in the heat and mass transfer phenomena. This model is described in details in a previous report (Léonard, 2009).

3.2 Rate-based model

3.2.1 Advantages of the rate-based model

The accuracy of the equilibrium model can be discussed. According to Abu Zahra (Abu Zahra, 2009), global results obtained with the equilibrium model are good as long as internal profiles of columns are not studied. It means that if internal profiles have to be precisely simulated, mass transfer and kinetics limitations can not be neglected anymore.

Figure 3.1 represents the different levels of complexity while modeling the reactive absorption (Lawal et al., 2008). The equilibrium model is at the bottom left extremity, i.e.

with poor accuracy for the calculation of mass transfer and chemical reaction rates. This model is described in Aspen Plus® by the Radfrac model for absorption columns. If we want to consider the mass transfer limitations, then we have to use another column model in Aspen Plus® that is called "Ratesep" column model. This Ratesep model implies calculations based on the mass transfer rate in the column packing at non-equilibrium conditions. For this model, packing data (mass transfer characteristics and geometry) have to be specified and a first design of the column can be performed.

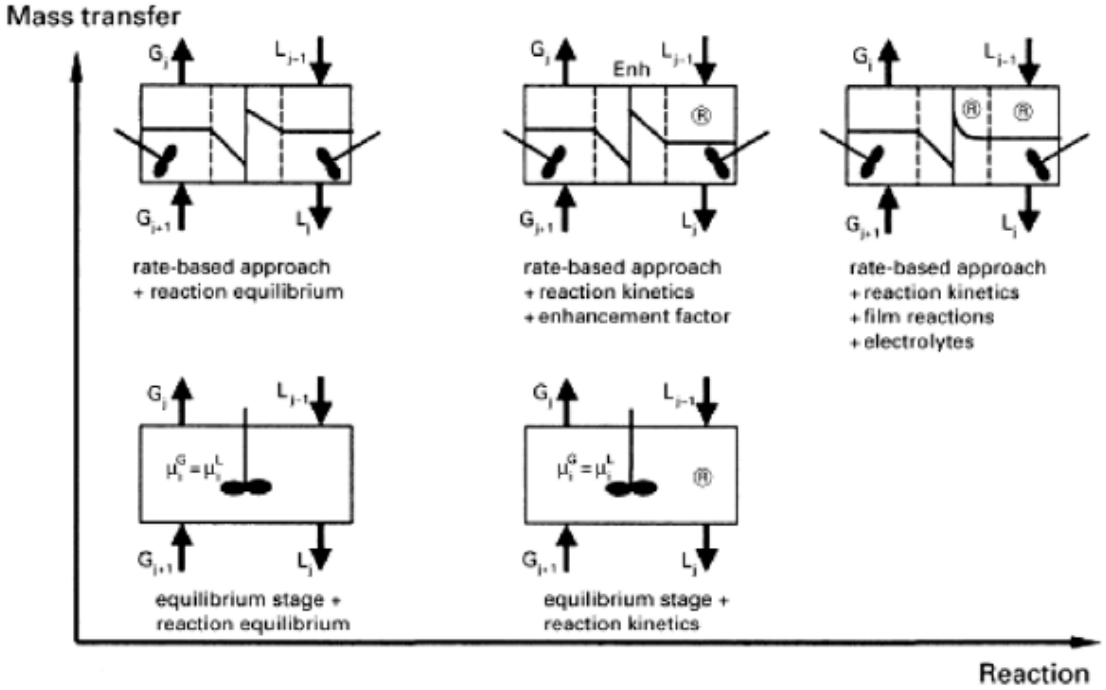

Figure 3.1: Complexity levels while modeling the CO_2 reactive absorption (Lawal et al., 2008)

Furthermore, it is also possible to consider the reaction kinetics in Aspen Plus®. When not considering the reaction kinetics, chemical reactions will only be taken into account through their equilibrium constant, as it has been done in the equilibrium model. In the rate-based model, kinetics constants of the absorption reactions have been taken into account.

Then, since the CO_2 absorption reaction in MEA is a rapid reaction (Dubois et al., 2009), the reaction takes place mainly in the liquid film, as shown in figure 3.2 (Léonard, 2009). In the model, the interface layer between liquid and gas has been divided into several sub-regions in order to improve simulation accuracy for film reactions. This is possible using the Aspen Plus® discretization option for the interface.

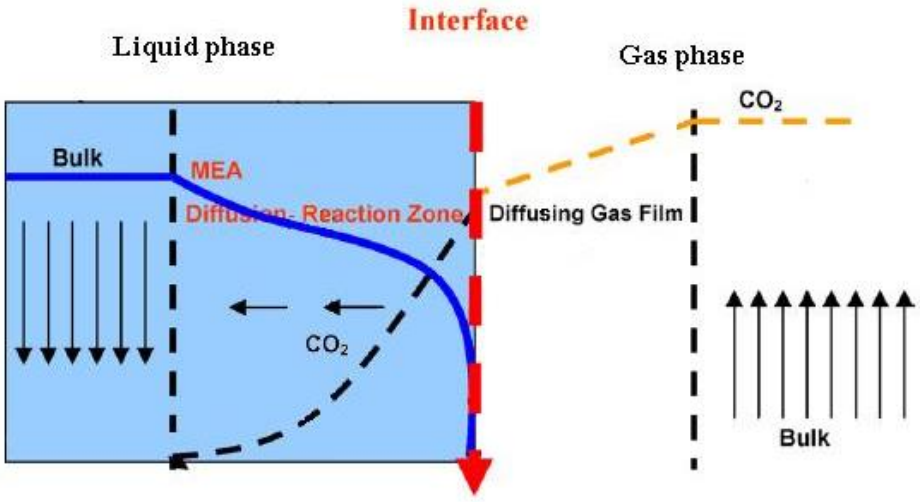

Figure 3.2: Representation of the gas-liquid interface

A detailed model for the calculation of electrolyte solutions is also available in Aspen Plus® and has been used in the present work (it was also used in the equilibrium model). The MEA-water system can be considered as an electrolyte solution since the amine can be protonated when diluted in aqueous solutions so that the resulting solution is conducting the current. The thermodynamical model we use for describing such solutions is the Electrolyte-NRTL model. It is based on the well-known NRTL model for the calculation of activity coefficients. Electrical considerations are added to the chemical model under the form of two main Assumptions (Aspentech, 2011):

- Assumption of repulsion for similar ions: the local composition of cations around cations is zero, and likewise for anions around anions.
- Assumption of local electroneutrality: the distribution of cations and anions around a central molecule is such that the net local ionic charge is zero.

Combining all those tools, the rate-based model is now located at the top right extremity on figure 3.1, which corresponds to the highest level of accuracy for mass transfer and chemical reactions calculations.

3.2.2 Description of the rate-based model

As already mentioned, in this second modeling approach, mass transfer limitations inside the columns have been taken into account, as well as chemical reaction kinetics. The rate-based simulation has been performed in Aspen Plus® using the RateSep block model with an electrolyte-NRTL model for the calculation of thermodynamic properties. Kinetics constants describing the CO_2 absorption reactions into MEA have been retrieved from the literature (Abu Zahra, 2009; Aspentech support 2010) and are presented in Table 3.1. These constants are used to calculate the reaction rate according formula (3.1).

$$r = k.e^{(-\frac{E}{RT})} \prod_{i=1}^{N} C_i^{\alpha_i} \qquad \text{Formula (3.1)}$$

Where
r = Rate of reaction
k = Pre-exponential factor
E = Activation energy

R = Gas law constant
T = Absolute temperature
N = Number of components
C_i = Concentration of component i
α_i = Exponent of component i

Table 3.1: Kinetics constants for the rate-based model

Kinetics reactions	k	E (cal/mol)
$CO_2 + OH^- \text{ --> } HCO_3^-$	4,32e+13	13249
$HCO_3^- \text{ --> } CO_2 + OH^-$	2,38e+17	29451
$C_2H_7NO + CO_2 + H_2O \text{ --> } C_3H_6NO^- + H_3O^+$	9,77e+10	9855,8
$C_3H_6NO^- + H_3O^+ \text{ --> } C_2H_7NO + CO_2 + H_2O$	2,7963e+20	17229,7817

However, some fast reactions are still described as equilibrium reactions. In this case, coefficients for the calculation of equilibrium constants using formula (3.2) come from the literature as well (Abu Zahra, 2009) and are presented in Table 3.2.

$\ln(K_{eq}) = A + B/T + C*\ln(T) + D*T$ Formula (3.2)

Where
K_{eq} = Equilibrium constant
T = Absolute temperature
A, B, C, D = User-supplied coefficients

Table 3.2: Constants for the calculation of equilibrium constants

Equilibrium reactions	A	B	C	D
$C_2H_8NO^+ + H_2O \text{ <--> } C_2H_7NO + H_3O^+$	-3,038325	-7008,357	0	-0,0031348
$HCO_3^- + H_2O \text{ <--> } H_3O^+ + CO_3^{2-}$	216,049	-12431,7	-35,4819	0
$2\ H_2O \text{ <--> } H_3O^+ + OH^-$	132,899	-13445,9	-22,4773	0

Further parameters for the calculation of the absorber and the stripper have been chosen based on the literature (Abu Zahra, 2009; Zhang et al., 2009) and reported in table 3.3. Packing data are from the Esbjerg pilot plant (Knudsen et al., 2009) as an example.

Table 3.3: Rate-based model parameters

Parameter	Absorber	Stripper
Packing	IMTP50, Norton, Metal	IMTP50, Norton, Metal
Packing height	17m	13m
Section diameter	1.1m	1.1m
Reaction condition factor [a]	0.5	0.5
Film discretization ratio	2	2
Model for film resistance	Discretized film in liquid phase, simple film in gas phase	Discretized film in liquid phase, simple film in gas phase
Interfacial area factor [b]	2	1.5
Flow model [c]	Mixed	Mixed
Discretization points for liquid film	5	5
Pressure drop	0,1 bar	0,3 bar

Stage number	17	23
Washing section	2-stages washing column	3-stages washing section inside the stripping column

[a] Ponderation factor between liquid bulk and liquid film conditions for the reaction rates calculation
[b] Interpolation factor for the calculation of the liquid – vapor interface
[c] Model used to describe the liquid condition at the interface boundary layer

Pressure drops in pipes have been neglected. Finally, in order to allow model convergence, a design specification has been implemented on the water balance in the process to insure that the water entering the process is in balance with the water exiting the process, and a make-up stream has been added to compensate for the water losses at the absorber washing section. Although it seems trivial, this specification is absolutely necessary to make the model converge. Indeed, water circulates in a nearly-closed loop, but some exchange happens between the aqueous solvent and the gaseous phase in the stripper and in the absorber. It is then necessary that the make-up water stream exactly compensates for the water losses. The design specification will also reduce the water make-up stream if necessary in order to prevent water accumulation in the process.

In the rate-based model, an important difference compared to the design specification implemented in the equilibrium model is that a purge stream has also been added that was necessary for the model calculations to converge, especially when an intercooler was added into the absorber. Indeed, the main effect of the intercooler is to reduce the mean absorption temperature (see section 3.3.2). There are then lower water losses at the absorber washing section and some water is even absorbed from the gas stream into the solvent, inducing a water accumulation in the process so that no steady state solution could be found. The only solution is to remove a part of the additional water. This blow-down is performed at a place where water is nearly pure, i.e. a part of the condensed water from the stripping column condenser is purged instead of being recycled to the stripping column.

3.3 Simulation results

The process optimization is based on two complementary approaches. In the first part of this section, process parameters having a large influence on the global process efficiency are identified and optimized. This sensitivity analysis has been performed by varying the studied parameter and keeping other parameters constant. Since the results of this study for the equilibrium model have already been published in a previous work (Léonard, 2009), they are now compared to the results obtained using the rate-based model. Then, in the second part, some process modifications implying additional equipment have been implemented in the rate-based model which is more accurate for the description of column internal profiles. In this optimization process, the comparison criterion is the thermal energy requirement at the reboiler of the desorption column, which composes the largest part of the total process energy requirement.

3.3.1 Sensitivity study of process parameters

In the previous work, six process parameters have been studied using an equilibrium model and their influence on the total energy requirement quantified (Léonard, 2009). Those parameters were the followings:

- Solvent flow rate
- Solvent concentration

- Solvent temperature at absorber entrance
- Stripping pressure
- Temperature approach at the lean-rich heat exchanger
- Condenser temperature at the stripper exit

The solvent concentration and the stripping pressure have a so large influence that it was possible to reduce the process energy requirement by more than 10% while optimizing those parameters. Moreover, it appears as essential to optimize the solvent flow rate, since there is clearly an nominal value at which the process should work. These three parameters have then be studied using the rate-based model and results are compared to the results obtained on the equilibrium model.

On the figure 3.3, we see that there is for both models a minimum in the curve of energy requirement in function of the solvent flow rate. In terms of solvent flow rate, the location of the minimum is approximately the same, but the energy requirement is higher in the case of the rate-based model. Since mass transfer and kinetics limitations are taken into account in the equilibrium model, it seems logical that this latest gives a higher value for the process energy requirement, since it is not so close to an ideal process as the equilibrium model is.

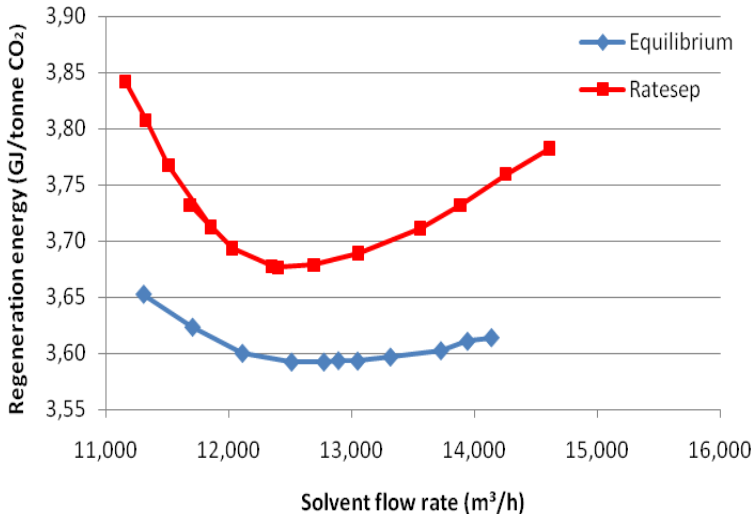

Figure 3.3: Influence of the solvent flow rate on the process energy requirement

Solvent flow rate values found in this study are in reasonable agreement with experimental results that attest the presence of a minimum in this curve. However, no accurate experimental data is available yet to confirm the location of this minimum.

Regarding the solvent concentration and the stripping pressure, Figure 3.4 a and b show that the curve obtained with the rate-based model (Ratesep block in Aspen Plus®) gives higher values for the process energy requirement than the curve obtained with the equilibrium model. This confirms the explanation that the equilibrium model does not take into account important limitations and is then closer to the ideal case (in which the process energy requirement corresponds to the bare thermodynamic value of the CO_2 desorption enthalpy).

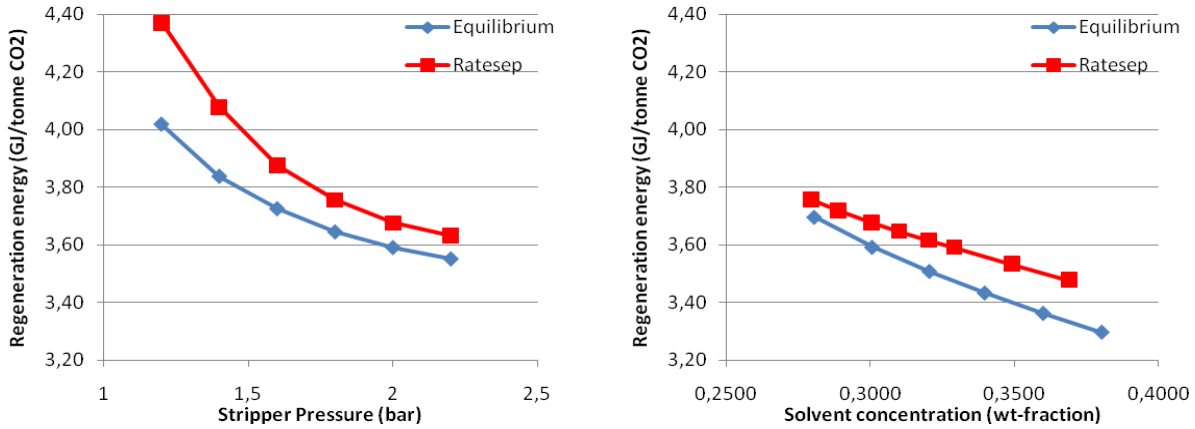

Figure 3.4 a and b : Influence of stripper pressure and solvent concentration on process energy requirement

On figure 3.4 a, it requires less regeneration energy to work at a stripping pressure higher than the atmospheric pressure. This is due to the strong dependence of the CO_2 partial pressure on the temperature (Leonard, 2009). When the pressure is increased, the temperature of the regeneration also increases, so that the CO_2 partial pressure rises proportionally more than the total pressure, and CO_2 is easier desorbed. On figure 3.4 b, the more concentrated the solvent, the lower the process energy requirement since the same mass flow of solvent can absorb a higher amount of CO_2 due to the higher amine concentration. However, those results don't take into account connected phenomena like solvent degradation at high temperature (related to high pressure in the stripper), additionnal compression costs at higher stripping pressure, increased corrosivity of concentrated solvent, …
Table 3.4 summarizes some results and compares the different options in terms of influence of the parameter on the process energy requirement related to the base case.

Table 3.4: Optimization of process parameters

	Stripper pressure	Solvent concentration	Solvent flow rate
Equilibrium model			
Base case value	1.2 bar	30 wt-%	15 m³/h
Optimum value	2.2 bar	37 wt-%	12.8 m³/h
Regeneration energy	-11.6 %	-8.2 %	-1.6 %
Rate-based model			
Base case value	1.2 bar	30 wt-%	15 m³/h
Optimum value	2.2 bar	37 wt-%	12.4 m³/h
Regeneration energy	-16.9 %	-5.4 %	-2.8 %

3.3.2 Model improvements

In the second part of the optimization process, some technical improvements that require additional equipment have been simulated. The simulation gives then an idea about the potential gain in process efficiency without having to add some new equipment often complex to an existing pilot installation.

Three main process improvements have been studied, using the rate-based model since it is more precise to describe column internals. Those process improvements are represented on

figure 3.5. In red, the lean vapor compression (LVC) consists in partially evaporating the regenerated solvent at the stripper exit and so to recover some energy of the lean solvent under the form of vapor. This vapor generated in the adiabatic flash evaporator at lower pressure is then compressed and sent back to the stripper where it acts as stripping steam and induces a reduction of the reboiler duty. Some water is added to this vapor to cool it down, so that vapor temperature does not exceed 125°C after compression. This vapor is composed of approximately 90wt-% water and 10wt-% CO_2. Nearly no MEA is evaporated.

The absorber intercooling process is represented in blue. A liquid stream is drawn out of the absorber and cooled before flowing back on the same stage. Since the absorption reaction is exothermic, this operation decreases the mean absorption temperature and thus improves the process efficiency.

Finally, in green, the split-flow configuration consists in partially regenerating a part of the solvent and sending it to the absorber at middle height. This partially regenerated solvent will absorb CO_2 in the bottom of the absorber, where the CO_2 partial pressure is still high. In the top of the absorber, where CO_2 partial pressure in the gas phase is lower, absorption occurs with better regenerated solvent.

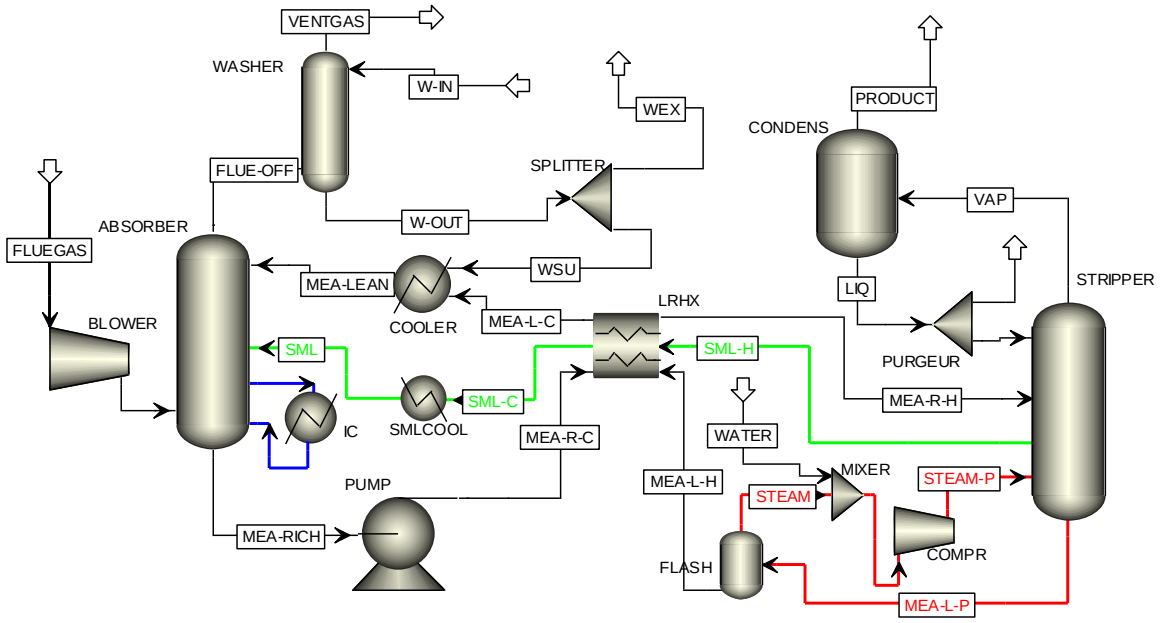

Figure 3.5: Process improvement on the CO_2 capture flowsheet

Each modification has been optimized. In the case of the LVC, the regeneration energy requirement has been driven from 3.68 down to 2.9 GJ/t CO_2, which corresponds to a reduction of about 21% thanks to this process modification. In order to take the energy supplied for compressing the lean vapor into account as well, the calculation has also been performed in term of exergy. It appears that the process exergy demand is globally reduced by 15%, from 1.35 to 1.15 GJ/t CO_2, considering that thermal energy is furnished to the process by steam at 170°C. When varying the adiabatic flash pressure, we can observe that the lower the flash pressure, the higher the energy savings.

Regarding the intercooling, the impact of the intercooler location on the regeneration energy requirement has been represented on figure 3.6. An intercooler placed at the bottom of the absorber corresponds to a flue gas pre-cooling.

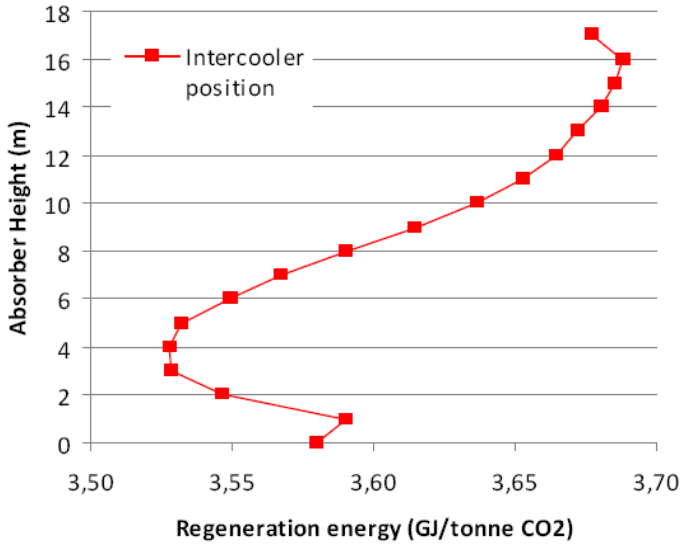

Figure 3.6: Influence of the intercooler location on the regeneration energy requirement

By adding an intercooler, the process energy requirement decreases from 3,68 GJ/t CO_2 to 3,53 GJ/t CO_2 in the optimal case, i.e. if the intercooler is located at the first third of the column (between stage 13 and 14). This corresponds to a gain of about 4%. The absorber temperature profiles represented on figure 3.7 for different intercooler locations confirm the decrease of the mean absorption temperature.

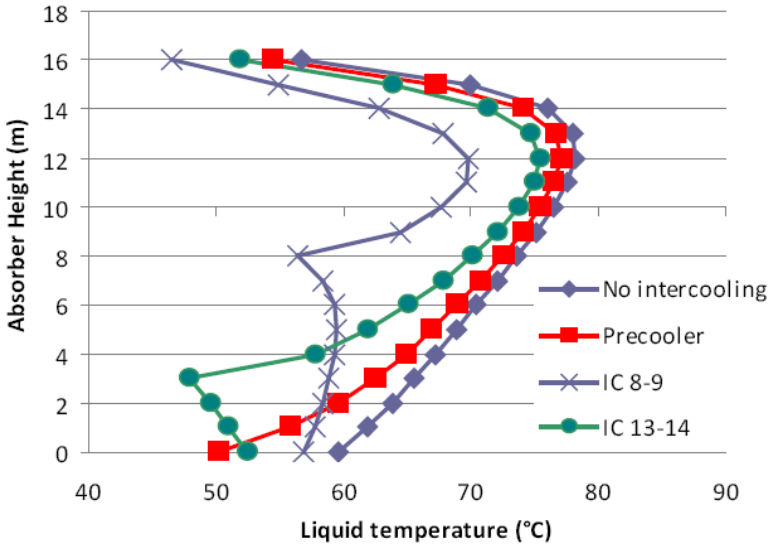

Figure 3.7: Absorber temperature profiles for different intercooler locations

It seems particularly important to have a low absorption temperature at the bottom of the absorber. Indeed, the mean temperature of the case where the intercooler is located between absorber stages 7 and 8 (IC 7-8) seems lower than in the case IC 13-14, but the better process efficiency is reached in this second case. It could be explained by the fact that the largest part of the absorption occurs in the lower third of the column due to the high CO_2 partial pressure in the gas phase in that region.

The third process modification, the split-flow configuration, is from an equipment point of view quite complex, because it requires a complex heat-exchanger able to manage numerous

streams. One quarter of the total solvent mass flow is side-drawn from the stripper column. This partially regenerated solvent is then injected into the absorber to perform the absorption in the region where the CO_2 partial pressure is high. The absorber return stage has been optimized and it appears on figure 3.8 that the optimal location is on the 11th stage.

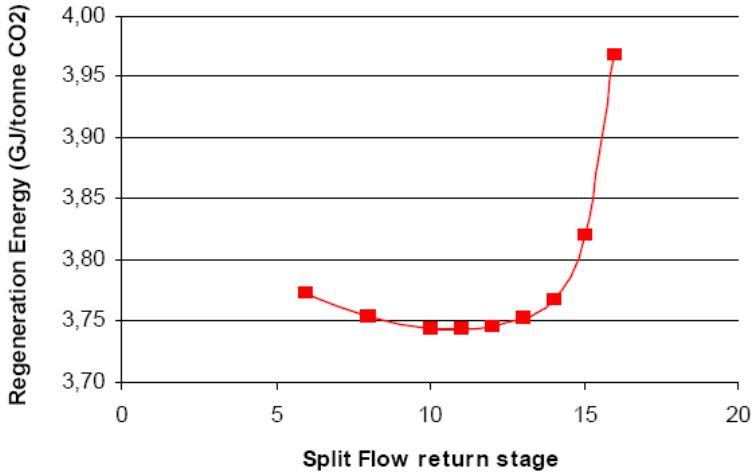

Figure 3.8: Determination of the optimal split flow return stage

Figure 3.9 shows the results of a sensitivity study performed by varying the total solvent flow rate in the split flow configuration. The split ratio has been fixed to 25% (i.e. 25% of the total solvent flow is sent to the absorber before being totally regenerated). We can see that there is once again a minimum in this curve. The shape of the curve is however slightly different from the case without this configuration (see figure 3.3). The minimum of energy requirement is reached at a solvent flow rate of 12.0 m³/h, which is close to the optimal value of 12.4 m³/h found in the model without split flow. The process energy requirement has decreased by 4%, from 3.68 to 3.53 GJ/t CO_2.

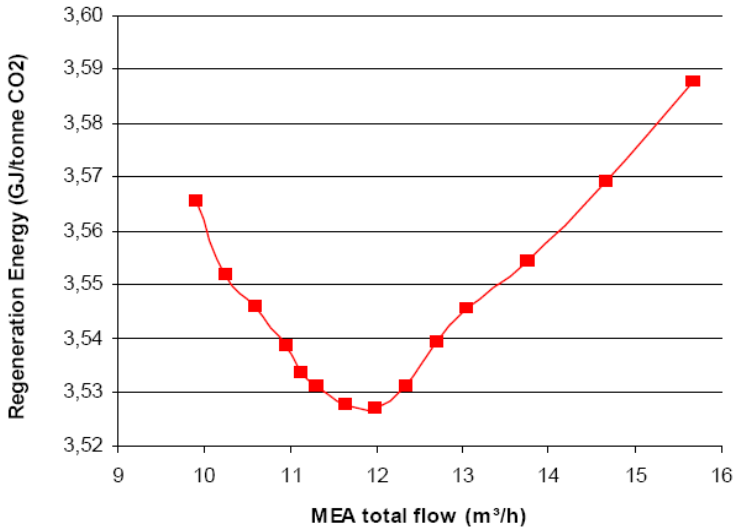

Figure 3.9: Optimization of the solvent flow rate in the split-flow configuration

Finally, table 3.5 summarizes the process modifications studied. The lean vapor compression is clearly the most interesting modification from a process efficiency point of view.

Table 3.5: Comparison of different process improvements

Process improvement	Lean vapor compression	Absorber intercooling	Split flow configuration
Gain in regeneration energy	-21 % (Exergy: - 14 %)	- 4 %	- 4 %

3.4 Perspectives

Many equilibrium and rate-based models are already available in the literature. The particularity of this model is that it has been developed to describe an existing pilot plant for which experimental campaigns will soon begin. As soon as data will be available, the model shall be validated, so that further developments can take place.

Since the goal of this PhD work is to establish a link between simulation and solvent degradation, further work will tend to include parameters that will allow a rough modeling of solvent degradation. According to the CO_2 and O_2 content of the flue gas, to the reboiler temperature in the stripper, to the presence of SO_x and NO_x in the flue gas, … the degradation rate will vary and its impact on the process efficiency will be studied.

The final objective of the model with degradation will be to perform a multi-objective optimization of the CO_2 capture process. For this purpose, it may be possible to transpose the rate-based model into Aspen Custom Modeler®, a program that will allow a better interaction of this model with other simulation tools. Indeed, this interaction is not optimized in Aspen Plus®. Other modeling tools like for instance Matlab® can be used to define an objective function. This objective function will consider process efficiency parameters (like the thermal energy requirement per ton of captured CO_2) as well as degradation parameters (like the cost of solvent replacement and solvent disposal). Combining both aspects, different possible optimum operating points will be proposed for the CO_2 capture process.

4 Degradation

According to Sexton (Sexton, 2008), solvent degradation is "*an irreversible chemical transformation of alkanolamine into undesirable compounds resulting in its diminished ability to absorb CO_2.*" Solvent degradation has a large impact on the carbon capture process efficiency. First of all, the solvent make-up is an important cost factor in the CO_2 capture process. During the second test campaign on the Esbjerg pilot in Denmark that has lasted for 500 hours, 720 kg MEA were consumed, which corresponds to a specific MEA consumption of 1.4 kg MEA per ton of captured CO_2[1] (Knudsen et al, 2009).

Then, the presence of degradation products affects the solvent properties, leading to the numerous problems listed below:

- Increase of the solvent viscosity, leading to a higher solvent pumping work.
- Decrease of the solvent absorption capacity, decreasing the process efficiency.
- Apparition of foaming and fouling problems in the mass transfer columns.
- Corrosivity of degradation products leads to an increased equipment corrosion. Since corrosion implies the release of metallic ions from the pipe walls into the solution, and considering that the degradation reactions are catalyzed by those metallic ions, the degradation reaction is self-sustaining.
- The environmental impact of degradation products has also to be considered (potential toxicity of degradation products, additional cost for the safe disposal of those products, …).

According to Abu Zahra, the additional costs due to solvent degradation could represent up to 35% of the capture direct operation costs, i.e. 4.78 million Euro per year in the case of a 600MWe coal-fired power plant (Abu Zahra, 2009).

The objectives of this PhD thesis regarding degradation are both experimental and theoretical. In association with the industrial partner Laborelec, the construction of a test rig for the study of accelerated solvent degradation under high pressure and high temperature conditions has been decided. The first objective is to get a more detailed comprehension of the degradation phenomena and to quantify the influence on degradation of different process parameters like temperature, pressure, gas flow rate and composition, …. Focusing on the degradation of 30 wt-% MEA, many experimental runs are performed in batch mode as well as in semi-batch mode, by which a gas continuously flows through the solvent solution. Different analytical methods are developed in order to characterize the results. Then, the second experimental objective is to test some alternative solvents systems, including the influence of corrosion and degradation inhibitors. Those results will be compared to the MEA base case. Based on the obtained experimental results, some parameters will then be implemented in the simulation model described in chapter 3. The third objective, this one theoretical, is to develop a model of the CO_2 capture process taking the solvent degradation into account.

This chapter dedicated to degradation is divided as follows. First, a literature review is presented in order to make an overview of the state-of-the-art on degradation. In section 4.2, the degradation test rig built at the University of Liège will be presented. The main elements of the experimental bench are described. Section 4.3 is devoted to the development of the analytical methods used to characterize the degradation, mainly liquid and gas

[1] This consumption may also be due to solvent losses resulting from MEA evaporation, entrainment and leakages but this is not certain since no MEA was detected in the flue gas emissions (Knudsen et al, 2009).

chromatography. The first results obtained from the degradation test rig are then presented and discussed in section 4.4. Finally, some perspectives are presented in section 4.5.

At the end of this report, in the annex part, some further information about the degradation test rig are presented. The detailed risk analysis for the experimental bench are reported in the annex as well as the experimental procedures for operating it. Both documents are written in French since their main use is to provide a useful help for the technical staff operating the bench.

4.1 Literature Review

First, the different degradation mechanisms are briefly explained in order to get a better comprehension of the problem, and the potential degradation products evocated in the literature are listed. Then, the main research groups and their achievements are described.

4.1.1 Degradation mechanisms

Different degradation mechanisms occur in the CO_2 capture process. Many studies have been performed to determine which mechanism plays the largest role, according to the reaction conditions (among others, see Bedell, 2009 and Lepaumier, 2008). The three main degradation mechanisms are the thermal degradation, the oxidative degradation, and the degradation under CO_2.

Thermal degradation occurs only at high temperature, when the solvent is heated up in the stripper reboiler for regeneration (~120°C). It also happens during the reclaiming process which consists in a distillation in order to separate the solvent from its degradation products. Thermal degradation is catalyzed by the presence of metal ions in solution (Bedell, 2009).

Oxidative degradation occurs through the solvent contact with oxygen that takes place especially in the absorber. Indeed, the flue gas contains approximately 6 vol-% of O_2, varying with the type of fuel fired in the power plant (gas or coal). The reaction of the amine solvent with oxygen has been showed to be catalyzed by the presence of metal ions as it was the case for thermal degradation (Bedell, 2009). Moreover, it implies most of the time a larger degradation extent than in the case of thermal degradation (Lepaumier, 2008). Oxidative degradation also occurs at lower temperature like the absorber temperature (~60°C).

The third main degradation mechanism occurs in the presence of CO_2 and implies irreversible reactions between the amine and CO_2. Since the role of the amine is to absorb CO_2, their contact is enhanced in the mass transfer columns, so that MEA carbamates ($C_3H_6NO_3^-$) are formed during the absorption. Those reactions are expected. However, it may sometimes happen that carbonate (HCO_3^-, CO_3^{2-}) and carbamate species further react, forming degradation products that can not be regenerated in the stripper. As in the case of oxidative degradation, the degradation under CO_2 may lead to larger degradation extent then by thermal degradation.

4.1.2 Degradation products

The main MEA degradation products that have been reported in previous studies are represented in figure 4.1 (Lepaumier, 2010). However, the presence of some of those degradation products marked in grey is more uncertain.

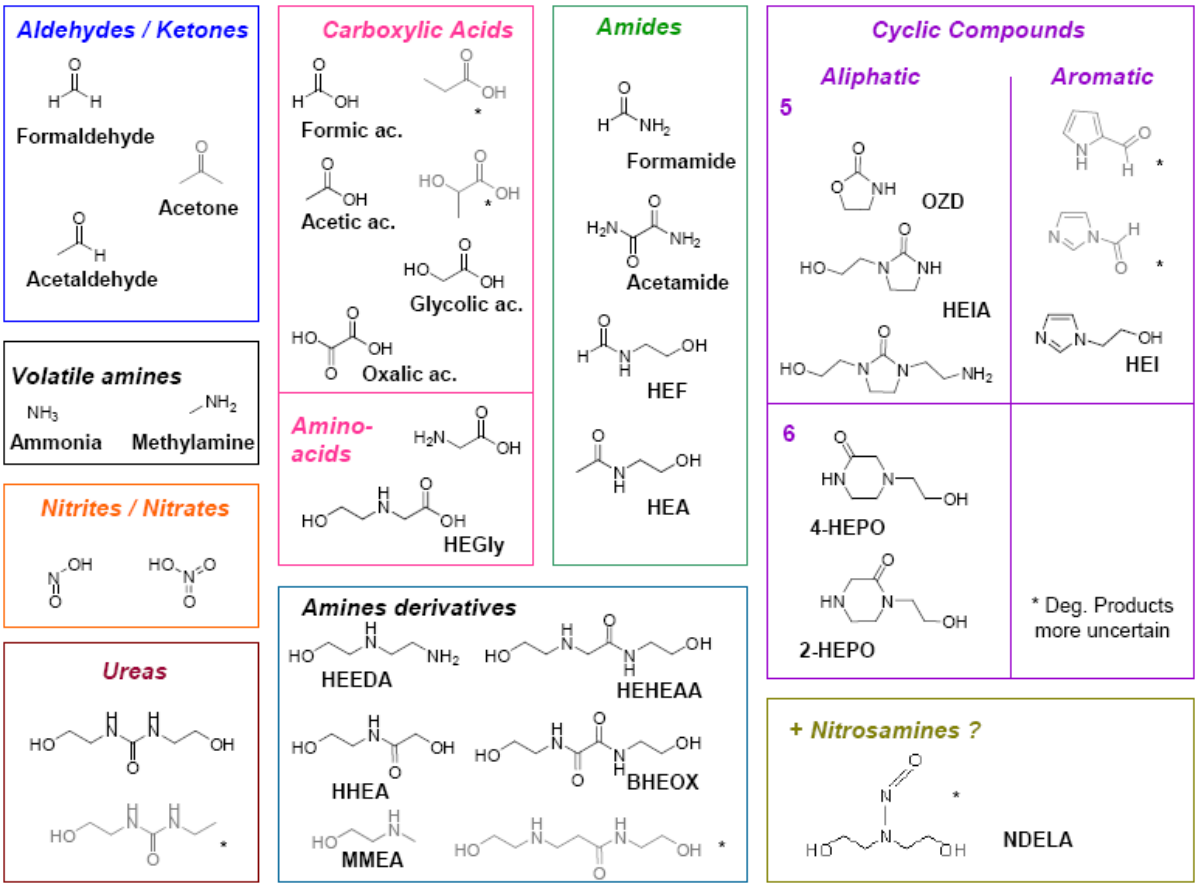

Figure 4.1: Degradation products of MEA

The formation of those products can in most of the cases be explained based on the mechanisms described in previous section. More information on the detailed formation mechanisms can be found in previously referred literature.

4.1.3 Research groups

Most studies concerning degradation of solvents employed for CO_2 capture have been published by two main research groups: the Regina University in Saskatchewan, Canada and the University of Texas at Austin in the USA. The third source consists in European research institutes working in the framework of European programs for CO_2 capture. The majority of those studies have been performed in the last ten years. Table 4.1 summarizes the research activity of those teams concerning solvent degradation with a particular focus on MEA degradation.

Table 4.1: Literature review of recent MEA degradation studies

Reference	Description	Volume	Gas feed mode	T (°C)	P (bar)	Solvent	Analysis	Run time
Supap et al., 2001	Kinetic law for MEA-degradation in function of solvent concentration, O2, Temperature and stirring	230ml	Discontinuous with gas feed to compensate for pressure losses	120-150	2,41-3,45 bar O2	MEA (2-11mol/L)	GCMS	2 - 12 days
Lawal and Idem, 2005; Lawal et al. 2005&2006	Influence of O2, CO2, MDEA-MEA-ratio, Temperature, amine concentration + Product formation mechanisms, Ecotoxicity	450ml		55-120	2,5 bar O2/CO2	MEA-MDEA blends (7-9mol/L)	GCMS (+HPLC from 2006)	6 - 22 days
Bello and Idem, 2005	Pathways of degradation reaction, influence of O2, CO2, Temperature, MEA concentration, ...	230ml		55-120	2,5-3,5 bar O2/CO2	MEA (5-7 mol/L)	GCMS	6 - 30 days
Supap et al. 2006	Analysis techniques: comparizon and methods	450ml		55-120	2,5-4,5 bar O2/CO2	MEA (5 mol/L)	GCMS, HPLC, CE	18-24 days
Bello and Idem, 2006	Influence of the corrosion inhibitor NaVO3 on Degradation kinetics	230ml		55-120	3,5-4,5 bar O2/CO2	MEA (5-7 mol/L)	HPLC	6-30 days
Uyanga and Idem, 2007	Influence of the corrosion inhibitor NaVO3 and of SO2 on kinetics. Kinetics model	450ml		55-140	2,5 bar $O_2/N_2/CO_2/SO_2$	MEA (3-7 mol/l)	HPLC	5-10 days
Supap et al., 2009	Kinetics data for O2 and SO2-induced Degradation	450ml		55-120	2,5 bar $O_2/N_2/CO_2/SO_2$	MEA (3-7 mol/l)	HPLC	6-13 days
Chi and Rochelle, 2000	Influence of CO2-loading and inhib (Fe, Bicine, EDTA) on NH3 production rate	500ml	5L/min Air/N2/Air+2%CO2	55	1	MEA (13-42 wt-%)	FTIR	up to 8 hours
Goff and Rochelle 2004; Goff, 2005; Goff and Rochelle 2006	Importance of O2-mass transfer and agitation rate, influence of Fe-Cu and of the presence of degradation products on degradation rate, Test of several oxydative degradation inhibitors for Fe-Cu catalysed degradation	550 g	Up to 8L/min Air/Air + CO2	55	1	MEA (6-85 wt-%)	FTIR	8- 17 hours
Sexton, 2008; Sexton and Rochelle, 2009	Test of different gas flow rate, influence of degradation catalysts (Fe, Cr-Ni, Cu, V) and inhibitors, test of MEA-PZ blends, amine screening	350-400ml	Low flow (100ml/min 2%CO2/98%02) and high flow (7,5 L/min Air/N2/2%CO2)	55	1	MEA (42 wt-%)	FTIR, IC (AC&CC), HPLC	12-15 days
Davis and Rochelle, 2009; Davis 2009	Dependance of Degradation rate on Temperature, Pressure and amine concentration. Thermal degradation of different amines, Kinetics model.	10ml	Batch +CO2	100-150	1-8	MEA (15-40wt-%)	IC (cationic), HPLC, MS	Few days to several months
Bacot et al., 2007	Degradation and corrosion screening for 20 amines	Not reported	Batch	140	5 bar O2/CO2/N2	Different amines	GC, GCMS, HPLC, IC	14 days
Notz et al., 2007	Degradation rate of primary, secondary amines, and activator (PZ).	350g	10 nml/min 40%N2, 30%O2, 30%CO2	90	1	Different amines	GC, RMN	14 days
Notz 2009	Solvent degradation induced by contact with gas, Castor 1&2, MEA	350g	10 - 20nml/min N2/O2/CO2	40-120	1-4	MEA	GC-FID	14 days
Notz 2009	Thermal degradation	7 ml	Batch	140-180	N2 atmosphere	MEA (30wt-%)	GC-FID	7 days
Knudsen et al., 2007	Results from test campaigns on Esbjerg pilot	~20m³/h	Plant conditions	up to 125°C	max 2 bar	MEA (30wt-%) +Castor1&2	Not reported	Several months
Captech, 2007	Degradation studies for the Captech program. Few details available.	100ml	350 ml/min N2/CO2/Air	150	1.2	Different amines	GC	Several months
Lepaumier, 2008; Lepaumier et al., 2008	Degradation Mecanisms and products for differents amines	100ml	Batch O2/CO2/N2/Air	140	20	Different amines	GCMS, RMN	2weeks

4.2 Description of the Degradation Test Rig at the University of Liège

The degradation test rig has been designed in order to perform degradation studies on classical and innovative solvents systems for post-combustion CO_2 capture. Since degradation reactions show slow kinetics rates, the objective is to accelerate this phenomena so that degradation can be observed in a shorter time range. This is why the degradation takes place in a stainless steel reactor so that high pressure and temperature conditions can be chosen. Moreover, it is possible to operate the test rig whether in batch or semi-batch operating modus, depending on the gas supply (respectively discontinuous or continuous). After describing the reactor, we will then present the gas supply system, the equipment to maintain the water balance in the reactor, the gas outlet system, and finally the control panel. Those elements are presented on figure 4.2.

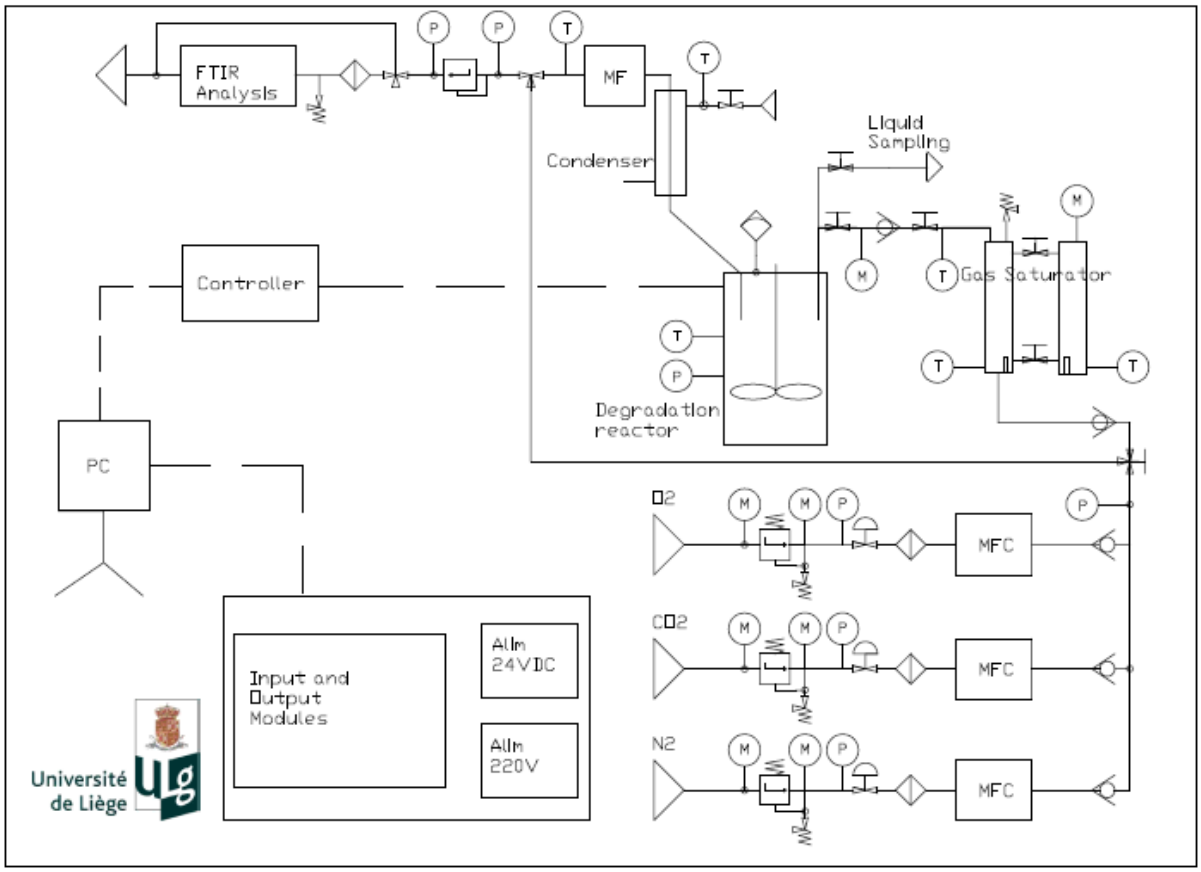

Figure 4.2: Flow sheet diagram of the Degradation Test Rig

4.2.1 Degradation reactor

The reactor has a capacity of 600ml and is totally made of T316 stainless steel (Figure 4.3 on the left). Its maximal operating temperature is 500°C and maximal pressure is 200 bar. It is operated with a hollow shaft agitator in order to enhance the gas-liquid contact (figure 4.3 on the right), so that reactions are not limited by physical kinetics: pressure is reduced in the agitator when it is rotating so that gas is aspired into the shaft and redistributed in the liquid at the bottom of the reactor.

Figure 4.3: Reactor and hollow shaft agitator

The heating is performed by a heat mantle, and controlled by the reactor controller (see section 4.2.5). Inside the reactor, different elements are present that are described on figure 4.4.

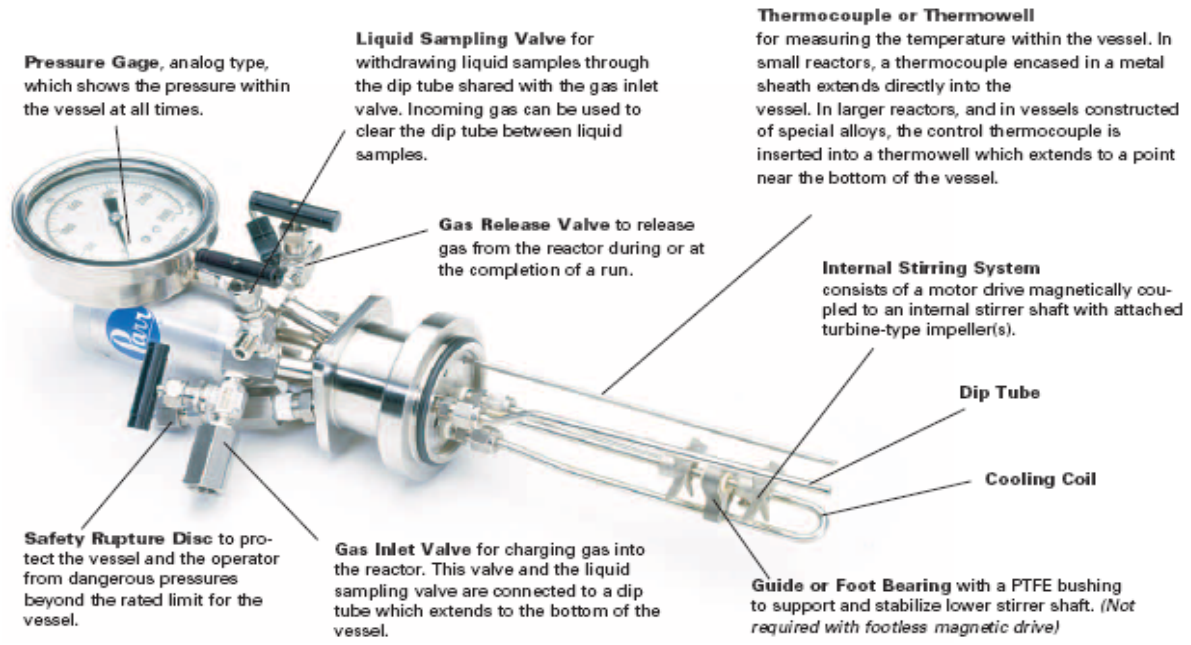

Figure 4.4: Description of the reactor head

4.2.2 Gas supply system

The reactor can be alimented with N_2, O_2, or CO_2. Four bottles and pressure regulator systems are attached to a bottle rack near the reactor, since compressed air is also needed for the regulation of pneumatic valves (Figure 4.5, on the left). However, keeping the existing configuration, other feed gases are also possible. The gas supply line also comports pressure transducers, security valves (controlled with compressed air), filters, mass flow controllers and check valves (Figure 4.5, on the right).

Figure 4.5: Bottle rack and gas supply

4.2.3 Water balance control

If the water balance is controlled, then the dry feed gas will be loaded with water before exiting the reactor, and the mass in reactor won't remain constant, nor solvent concentration. The solution that has been developed consists in a saturation of the feed gas before the reactor, followed after the reactor by a condensation of water out of the outlet gas (Figure 4.6, respectively left and right). Saturation and condensation are performed at the same temperature, so that the gas inlet and outlet occurs at the same temperature and same water content (since we consider that the gas remains saturated with water).

Figure 4.6: Water balance control (saturator and condenser)

The temperature for the gas inlet and outlet ranges between 15 and 70°C. The pressure can be that of the reactor, i.e., it can reach up to 25 barg. A sample cylinder makes the sampling of condensate at the reactor outlet possible.

4.2.4 Gas outlet

The reactor is located at direct proximity of a FTIR analyzer for gas (see section 4.3). The gas outlet is directly connected to this analyzer via a 3-ways valve. For calibration purposes, the gas supply can also be directly connected to the FTIR analyzer, bypassing the reactor. The connecting schema of the gas outlet is represented on figure 4.7.

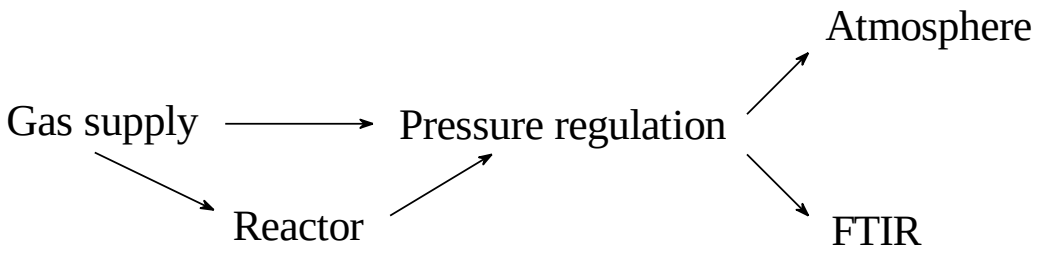

Figure 4.7: Connecting schema of the gas system

Directly after condensation, a Coriolis flow meter measures the outlet gas rate. A manual backpressure regulator regulates the pressure in the reactor and acts like a security valve that only opens when the pressure in the reactor overcomes a precise value. The line between the backpressure regulator and the FTIR analysis is heated thanks to a heating rope to prevent any water from condensing in the tubing if the temperature is too low.

4.2.5 Control Panel

There are two controlling systems related to the degradation test rig. First, a controller box has been furnished with the reactor and controls the reactor main parameters (temperature, agitation rate). These parameters are recorded in the PC as well as the reactor pressure.

The second controlling system is a Labview® application. Labview® is a software developed by National instrument. This software is controlling the mass flow controllers, the heating rope and heating cartridges used in the gas saturator, and the security valves. It also acquires data from temperature and pressure sensors, and from mass flow controllers. Different alarms are implemented in that software, so that if recorded values get out of range because of installation break-down or current failure, the software shuts the installation safely down.

4.3 Analytical methods

To follow degradation studies, analytics consideration is of high importance. In this section, different apparatus and methods are described.

First, concerning the liquid phase, High-Pressure Liquid Chromatography with Refractive Index Detector (HPLC-RID) is presented. The objective of this method is to quantify the MEA concentration. The second method described is the Gas Chromatography with Flame Ionization Detector (GC-FID). The goal of this method is to identify the degradation products (that are usually badly separated using liquid chromatography HPLC) and to quantify them.

Then, Fourier Transform Infra Red (FTIR) analysis for the gas phase is discussed. Indeed, in the semi-batch experiments, a gas mix is bubbling through the amine solution. The objective of the FTIR is to characterize the gaseous emissions occurring during the degradation experiments.

Finally, some analyses have been performed in other labs. First, a following of the metal ions present in solution has also been performed by the Laboratory of Hydrogeology at the University of Liège in order to get some insight on corrosion phenomena. Indeed, it is important to know the exact concentration of metal ion since they may have an influence on the degradation mechanisms (see section 4.1.1). Then, a Karl-Fischer titration has been

performed by the Laboratory of Coordination and Radiochemistry of the University of Liège. The objective of this analysis is to determine the water content of the amine solution at the end of the degradation experiment in order to give some complementary information about the water mass balance in the degradation reactor.

4.3.1 High-Pressure Liquid Chromatography (HPLC)

The most important objective is to separate MEA from its degradation products, so that it will be possible to determine its concentration. HPLC is a very common analysis tool for the separation of compounds with different polarity.

The apparatus used is represented on figure 4.8. It is composed of a Water 515 HPLC pump, a Merck T-6300 column thermostat, a Waters 410 differential refractometer which measures the change of the refractive index in the solution and a PowerChrom 280 data acquisition unit combined with the PowerChrom software. A Merck Hitachi L-4200 UV-VIS detector has also been used in some experiments.

Figure 4.8: HPLC apparatus

The principle of this method consists in injecting a liquid sample in a column where the different components are eluted with different retention times, according to their affinity with the column stationary phase. In the present work, columns with reverse phase (hydrophobic stationary phase) have been used. With such columns, polar compounds elute first and non-polar compounds are retained on the column. Since MEA and most of its degradation products are very polar compounds, they elute quite rapidly.

The sample is diluted with HPLC grade water (distillated water filtrated on 0,22µm cellulose acetate filters and degassed for 5 minutes under vacuum) in proportion 1:10. Using a syringe, 100µl of sample is injected in the column thermostat. The injector loop volume equals 20µl, this is the sample volume that really reaches the column. A guard column is used with the Macherey-Nagel columns so that the sample is filtrated before it reaches the column.

In order to optimize the separation of MEA with its degradation products, three different HPLC columns have been tested for the quantification of MEA. They are listed in order of increasing stationary phase polarity:

- HPLC column C18 Pyramid: a classical C18 column with OH groups end-capping;
- HPLC column Nucleosil SA: a column with -SO_3Na groups (cation exchanger);

- HPLC column Kinetex Hilic: a reverse-reverse phase that implies strong polar interactions with the sample.

4.3.1.1 HPLC column C18 Pyramid

The first column described here is a classical C18 column from the company Mascherey-Nagel. The characteristics of this column are listed in Table 4.2.

Table 4.2: Characteristics of the C18 Pyramid HPLC column

Column name	C18 Pyramid
Brand	Macherey-Nagel
Phase	Octadecyl
Separation mechanism	Polar selectivity
Carbon content	14%
Length	125mm
Internal diameter	4,6mm
Particule size	5µm

The phase recovering the column walls is represented on figure 4.9. Normal C18 phases are not stable in the presence of aqueous solvent. The polar OH group is used as phase end-capping, so that the column is stable with 100% aqueous solvents, which is the particularity of C18 Pyramid column.

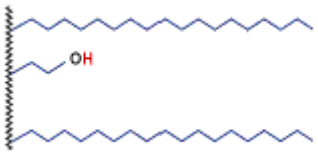

Figure 4.9: C18 Pyramid stationary phase

Different eluents (or mobile phase) were tested: methanol-water solutions, acetonitrile-water solutions and aqueous phosphate buffer solutions. The spectra obtained with an aqueous solution of methanol or acetonitrile in varying proportions gave bad base line spectra and no separation. A third eluent has been tested based on literature data (Kaminsky et al., 2002; Supap et al., 2006). This eluent consists in a phosphate buffer solution ([KH_2PO_4] = 0,08M; pH stabilized at 2,6). In this case, the separation has been slightly improved but was still clearly insufficient.

4.3.1.2 HPLC column Nucleosil SA

The second column described here is a Nucleosil 100-5 SA column containing a strong cationic exchanger (sulfonic acid) as stationary phase (Macherey-Nagel, Düren, Germany). This column has been used in previous studies concerning amine degradation (Kaminsky et al, 2002; Supap et al, 2006). Figure 4.10 describes the stationary phase of this column. Its characteristics are presented in table 4.3.

Figure 4.10 : Nucleosil SA stationary phase

Table 4.3: Characteristics of the Nucleosil SA HPLC column

Column name	Nucleosil SA
Brand	Macherey-Nagel
Phase	Sulfonic acid modified silica
Separation mechanism	Strong cation exchange interactions
Carbon content	6,5%
Length	250mm
Internal diameter	4mm
Particule size	5µm

Here again, the same eluents as before were tested: methanol-water solutions, acetonitrile-water solutions and aqueous phosphate buffer solutions. With the methanol-water and acetonitrile-water solutions, poor results have been observed regarding the base line of the spectra and the peak separation, mainly due to tailing problems. The phosphate buffer eluent was the only one that gave acceptable results, even if the separation was still relatively poor.

The method that has finally been used for quantifying the MEA in degraded amine samples has been developed in accordance with previous literature studies (Kaminsky et al., 2002; Supap et al., 2006), that recommend the use of a phosphate buffer mobile phase. After preparing a 0,05M solution of KH_2PO_4 by weighting of the salt, the pH has been set to 2,6 by adding some concentrated phosphoric acid (min 89 wt-%). The eluent was then filtered using 0,22µm cellulose acetate filters and finally degassed 5 minutes under vacuum.

The phosphate buffer has two main advantages. First, it stabilizes the pH at the desired value in the buffer domain (close to the pKa of KH_2PO_4 which is equal to 2,148). This is important to have the right form of the interest compounds in solution. Since the pKa of MEA is approximately 9,5, the amine is completely ionized during the analysis, so that only one form of MEA is present in solution.

The calibration curve obtained with this method is represented on figure 4.11. We can see that this curve seems quite reliable with more than 99% precision. However, it has been obtained for pure MEA diluted with distillated water.

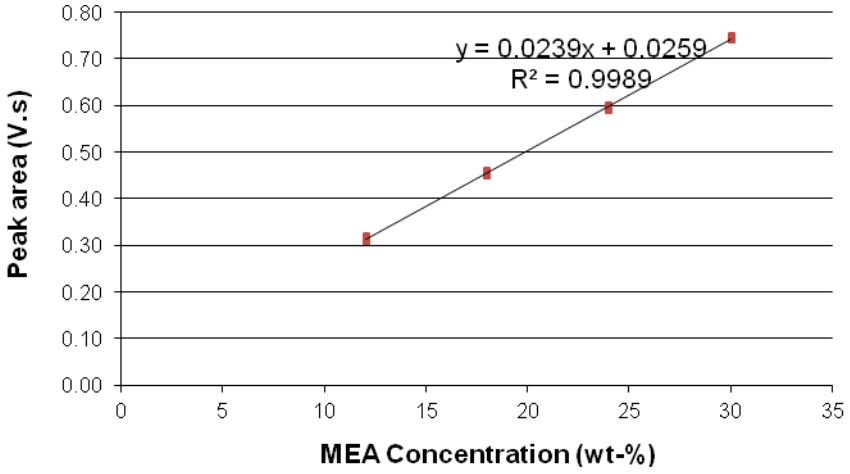

Figure 4.11: HPLC calibration curve for MEA

In the case of degraded solutions, the separation is still quite poor to precisely quantify MEA. Different parameters have been tested in order to improve this separation: buffer concentration, pH, column temperature, eluent mass flow. However, the spectra obtained for degraded solutions still presented rather poor separation and bad peak shape as to be observed on figure 4.12.

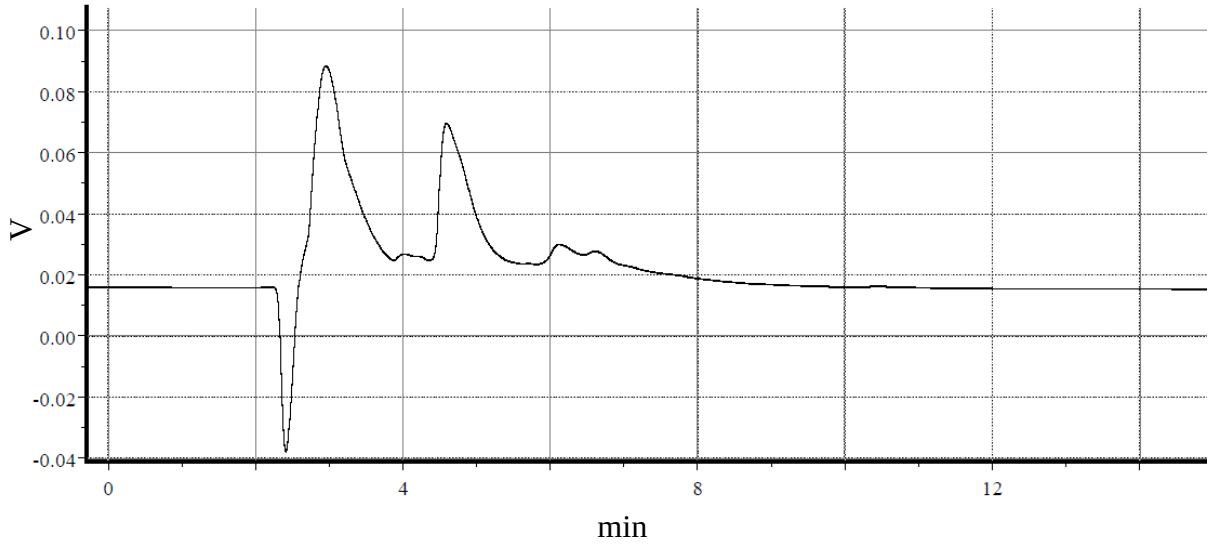

Figure 4.12: HPLC spectra of degraded MEA, Nucleosil SA column

4.3.1.3 HPLC column Kinetex HILIC

In order to improve the separation, a third column has been tested that is functioning in HILIC mode. HILIC stands for Hydrophilic Interaction Liquid Chromatography. It means that the elution time of a component is proportional to its polarity (and inversely proportional to the polarity of the mobile phase). Since amine components are very polar, this mode of operation may enhance the separation of the components. Figure 4.13 represents the HILIC stationary phase.

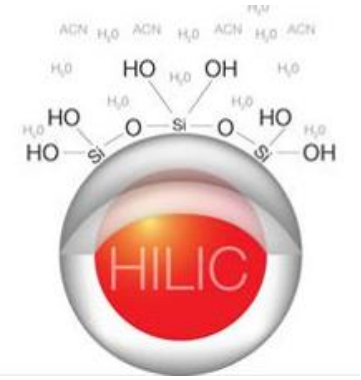

Figure 4.13 : HILIC stationary phase

Moreover, the Kinetex technology developed by the company Phenomenex uses stationary phase particles of lower size than classical HPLC stationary phases (see Table 4.4, particle size diameter is 2,6µm instead of typically 5µm). This new technology reduces the mass transfer limitations inside the columns, so that the separation efficiency is increased.

However, the counter-pressure of the HPLC system rises now up to 400 bar (it usually equals 200 bar in classical reverse-phase HPLC).

Table 4.4 : Characteristics of the Kinetex HILIC HPLC column

Column name	HILIC
Brand	Phenomenex
Phase	Unbounded silica
Separation mechanism	Hydrophilic interactions
Carbon content	0%
Length	150mm
Internal diameter	4,6mm
Particule size	2,6µm

In the case of the HILIC column, it is necessary to work with acetonitrile-water solvent, since water is a too polar solvent. In this case, the phosphate buffer does not seem to be a good eluent because of the bad miscibility of an aqueous KH_2PO_4 solution into acetonitrile. The alternative consists in an ammonium acetate aqueous solution diluted with water. First results presented on figure 4.14 show a better peak shape with less tailing in comparison with figure 4.12. Furthermore, the detector response is higher at the same dilution rate of the sample (1:10). However, the separation has still to be improved. Eluent optimization procedure is still in progress.

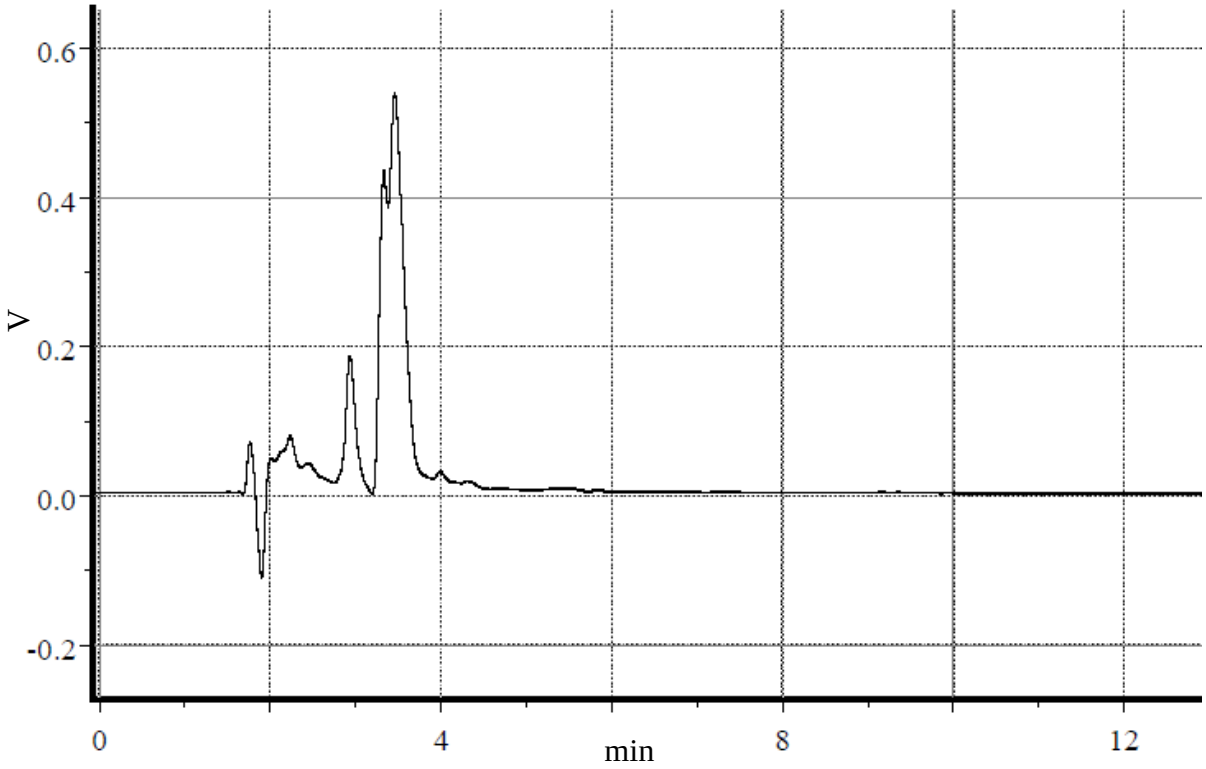

Figure 4.14: HPLC spectra of degraded MEA, Kinetex HILIC column

4.3.2 Gas Chromatography (GC)

The objective of the gas chromatography analysis is to identify and quantify the amine degradation products. The GC apparatus used for the analysis is a GC 8000 Series, made by Fisons Instruments. It is represented on figure 4.15. The software employed is the ChromCard Software.

Figure 4.15: Gas chromatograph

4.3.2.1 Method

The principle of the GC is the same as for the HPLC: a liquid sample is injected in a column where the different components are eluted with different retention times, according to their affinity with the column stationary phase. The difference is that the sample will be first vaporized before being eluted in the chromatography column.

Before the injection, the sample is first diluted with HPLC grade water (distillated water filtrated on 0,22µm cellulose acetate filters and degassed for 5 minutes under vacuum) in proportion 1:50. Using a syringe, 1µl of sample is injected in the injection cell which is heated at 280°C. The carrier gas (that replaces the eluent) is Helium. It flows continuously through the column and its pressure is kept constant at 0,6barg. The detector is a Flame Ionization Detector (FID) heated at 300°C.

The chromatography column is a capillary column OPTIMA-35 MS from Macherey-Nagel. Its characteristics are presented in table 4.5.

Table 4.5 : Characteristics of the OPTIMA-35 MS GC column

Column name	OPTIMA-35 MS
Brand	Macherey-Nagel
Phase	Cross-linked sylarene phase

Separation mechanism	Polar selectivity
Polarity Index	35 % Phenyl / 65 % Methyl-Polysiloxane
Length	30 m
Internal diameter	0,25 mm
Film thickness	0,25 µm

The column is set in an oven whose temperature is varying according to the temperature program encoded by the operator. The whole program lasts for 60 minutes, performing the following steps:

- T_1 = 35°C during 2 minutes, then the temperature increases by 7°C/min
- T_2 = 140°C, then the temperature increases by 5°C/min
- T_3 = 240°C during 8 minutes, then the temperature increases by 10°C/min
- T_4 = 300°C during 9 minutes.

4.3.2.2 Standards samples

In order to recognize the degradation products, the most frequent degradation products described in section 4.1.2 have been injected in the gas chromatograph. The figure 4.16 represents the chromatogram of those different standards. Table 4.6 lists those components in order of elution in the GC column. Their retention time is indicated as well.

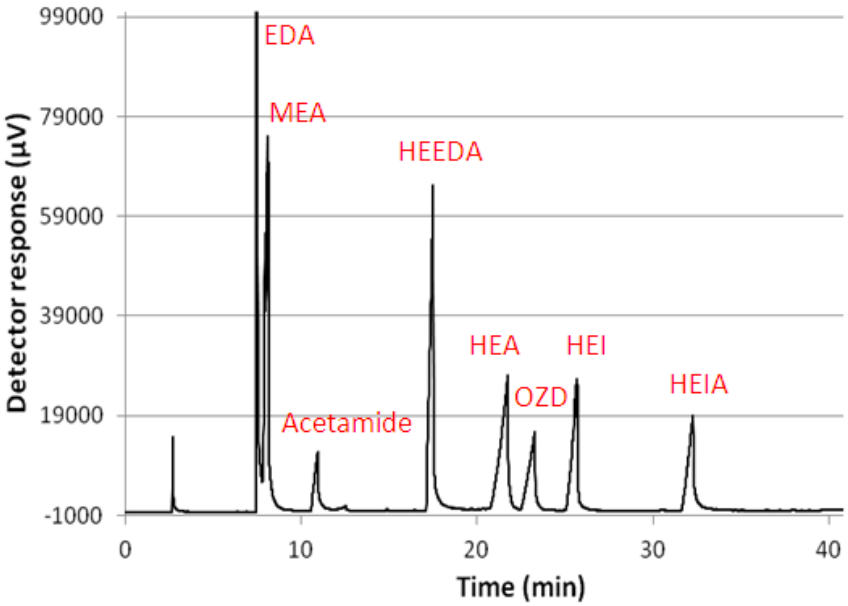

Figure 4.16: GC spectrum of the main standards

Table 4.6: GC Characteristic of standard degradation products[2]

Compound	Elution interval (min)
EDA	7.45 – 7.78
MEA	7.78 – 8.63
Acetamide	10.59 – 11.22
HEEDA	17.11 – 18.14
HEA	20.79 – 22.03
OZD	22.55 – 23.51

[2] An abbreviations list is available in the annex.

HEI	25.09 – 25.93
HEIA	31.67 – 32.69

4.3.2.3 Calibration curves

The calibration curves for MEA have not been realized yet. It appears that the use of an internal standard considerably reduces the error on the MEA quantification. 2-Methoxyethanol (1 wt-%) is used as an internal standard. Figure 4.17 shows a spectrum in which the internal standard is present. The method development is still under progress. The internal standard elutes during the time laps 6,25 - 6,86 minutes, approximately one minute before MEA, so that both peaks are well separated.

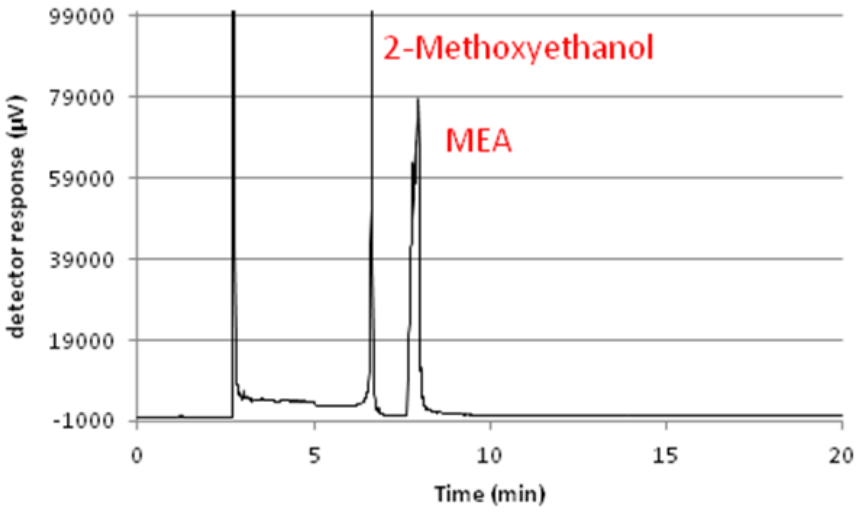

Figure 4.17: GC spectrum of MEA with internal standard

4.3.3 Fourier Transformed Infra Red analysis (FTIR)

The objective of the Fourier Transformed Infra Red spectrometer is to perform an analysis of the gas phase emitted during the degradation reaction. Since some degradation products are gaseous, the gaseous phase has to be analyzed to get a complete overview on degradation reactions. One of the major oxidative degradation products of monoethanolamine is indeed ammonia, which is emitted as a gaseous product (Chi and al, 2001; Knudsen et al, 2009). Thanks to the FTIR analyzer, it is possible to follow the degradation rate related to ammonia. The objective is to follow the concentration of water, CO_2, ammonia and MEA in the gaseous emissions.

This apparatus detects the infrared length waves that are absorbed by the sample. According to the chemical bonds of the components presents in the sample, it is possible to identify the components and to quantify them relatively to reference samples.

The FTIR is represented on figure 4.18. It is a 6700 Nicolet FTIR with a 200 ml gas cell (KBr window, 2 meter ray pathway length). The resolution of the analyzer reaches 0,125 cm^{-1}. The software related to the spectrometer is called Omnic 8.

Figure 4.18 : FTIR analyser

4.3.3.1. Standard spectra

In order to obtain reference spectra of liquid standard like water, MEA or NH_3, it has been necessary to vaporize those elements, so that only a vapor phase reaches the FTIR analysis cell. The vaporization occurs on a plate heated at 100°C. The liquid solution (respectively water, NH_3 in water, MEA in water) is contained in a syringe. The syringe is attached to a syringe pump, so that the flow rate of injected solution can be precisely controlled. While the liquid is injected through a septum on the heated plate, dried air is flowing over the heated plate, entraining the vaporized liquid sample to the FTIR analysis cell. Figure 4.19 represents this installation.

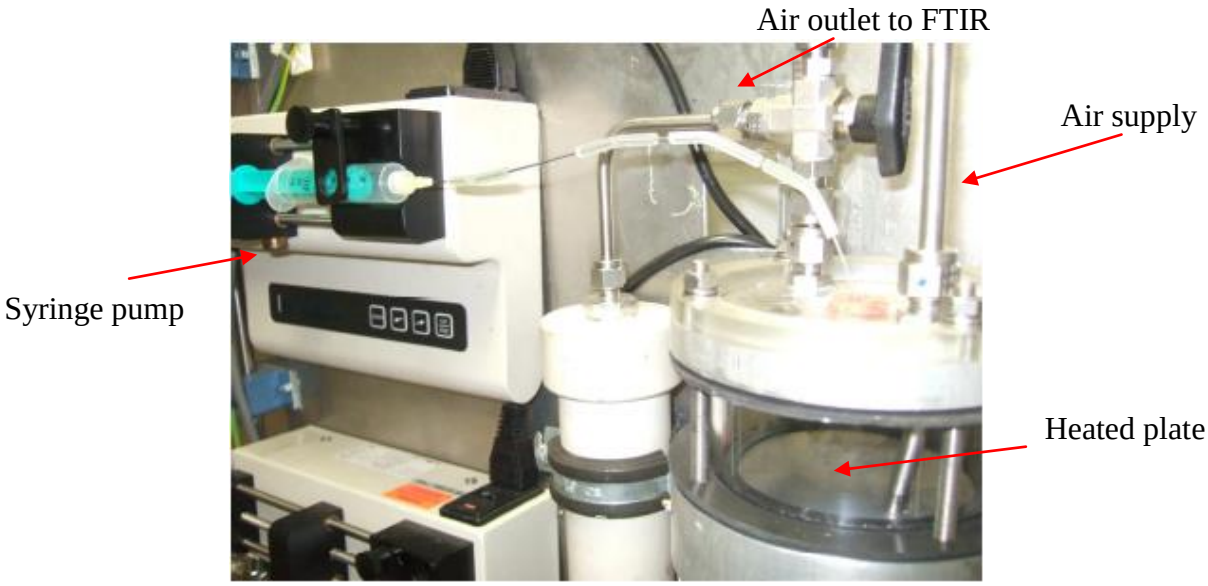

Figure 4.19: syringe pump and heated plate

Thanks to this installation, it was possible to analyze the IR spectrum of liquid standards. Each compound has one or several characteristic wavelengths at which the light is absorbed by the internal bonds. The presence and the concentration of a particular compound in the gaseous emission can be determined by observing a characteristic wavelength interval. The characteristic intervals for the studied compounds are presented in table 4.7.

Table 4.7: Characteristic absorption wavelength for FTIR analysis

Compound	Wavelength interval (cm^{-1})
CO_2	926 – 1150
MEA	2700 – 3200
H_2O	3200 – 3401
NH_3	910 – 1150

However, some spectral regions are interfering. That's why the biggest peaks associated to a compound are rarely chosen as characteristic wavelength regions. It is the role of the FTIR analysis to distinguish the different compounds based on calibration spectra. The different compounds listed in table 4.7 have been identified on FTIR spectra obtained on test samples. Figure 4.20 shows a spectrum of a CO_2 – water solution.

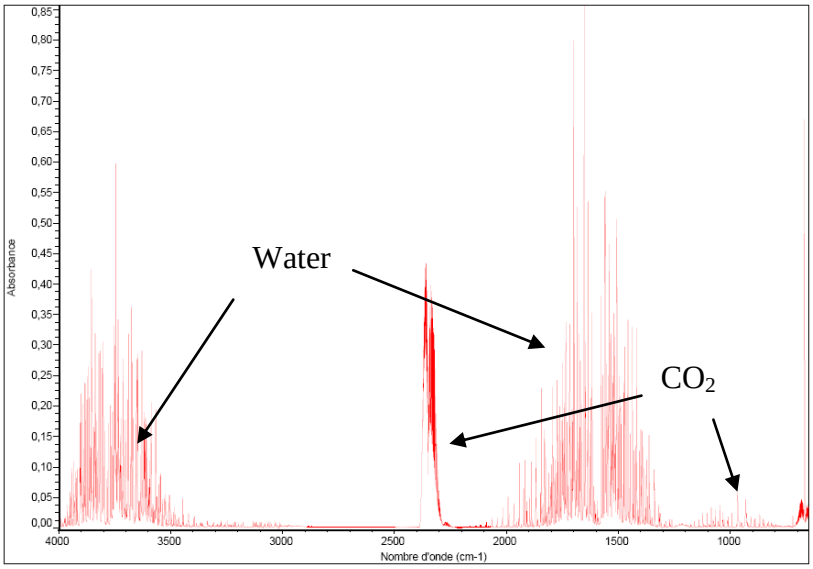

Figure 4.20: FTIR spectrum of a CO_2-H_2O sample

Figures 4.21 and 4.22 are showing respectively calibration spectra for MEA and NH_3.

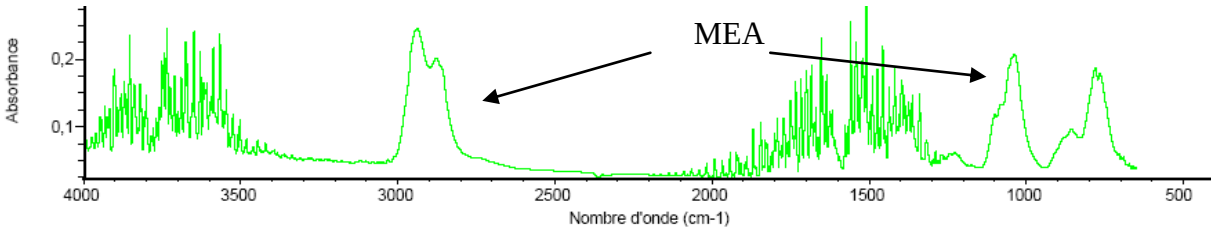

Figure 4.21: FTIR spectrum of a MEA-H_2O sample

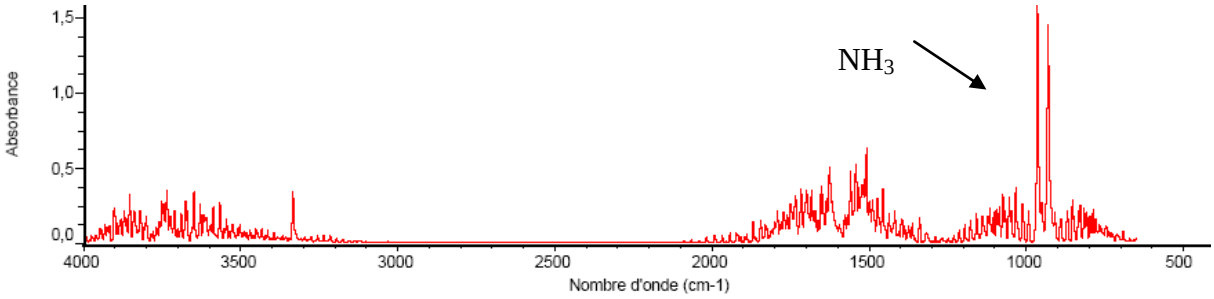

Figure 4.22: FTIR spectrum of a NH_3-H_2O sample

4.3.3.2 Calibration curves

The quantification of the main gaseous compounds (H_2O, MEA, NH_3, CO_2) using FTIR analysis is still in progress and should be achieved by the end of 2011.

4.3.4 Ion analysis

Parallel to analytical means developed internally in the framework of this PhD thesis, some samples have been sent to the Laboratory of Hydrogeology of the University of Liège for analysis. Since the MEA solution is corrosive, the reactor can be damaged during the degradation experiments. It has been observed that the stainless steel surface is modified to a certain extent due to corrosion. In order to follow this phenomenon and to prevent the corrosion from getting really problematic, the amount of ions present in the solution is regularly controlled. The objective is to assess the evolution of the corrosion in the reactor. Moreover, it may probably be possible to draw some relations between the degradation conditions, the obtained degradation products, and the metallic ions analysis. Those relations could give an insight on corrosion caused by the degradation products. Table 4.8 lists the analyzed ions and the employed analytic methods for their quantification.

Table 4.8: Analysis methods of ions

Ion	Method
Fe	Atomic absorption
Cr	Atomic absorption
Ni	Atomic absorption
Si	Atomic absorption
F	Capillary electrophoresis
Cl	Capillary electrophoresis

Iron, chromium and nickel are constituents of the T316 stainless steel. They are good indicators to follow the corrosion. Moreover, some studies have shown that those ions can have catalytic effect on solvent degradation (Sexton and Rochelle, 2009). Silicone has been found in some sample but its origin remains unknown. Fluorine and Chlorine have large effects on metal corrosion. Hence, their concentration will be systematically measured.

4.3.5 Karl-Fischer titration of water

The objective of the Karl-Fischer titration is to determine the water content of a degraded amine sample, and to relate it to the mass loss observed during the experiment in order to

characterize the water balance. The principle of this method is a chemical titration based on the reaction of sulfur dioxide and iodine in the presence of water:

$$2\ H_2O + SO_2 + I_2 \rightarrow SO_4^{2-} + 2\ I^- + 4\ H^+$$

As long as water is available in the sample, it reacts with SO_2 and Iodine (this last one is added progressively to the sample). The titration end point is detected by potentiometry as soon as some I_2 is present in excess in the sample. In the presence of an alcohol, the reactions are slightly different, but the principle remains the same.

Each amine sample has been diluted 1:20 with Ethanol (*per analysis* quality). 100µl of the diluted solution have been titrated using a 831 KF Coulometer Metrohm apparatus.

4.4 Results summary of the first tests performed

In this section, the first results obtained on the degradation test rig are presented. The objective of the degradation test rig is to get more experimental data on accelerated amine solvent degradation. The solvent tested is 30wt-% MEA. The influence of process parameters like temperature, pressure, gas flow rate and composition is first studied. Different operating modes are possible: the test rig can be operated in batch as well as in semi-batch mode, in which case a gas continuously flows through the solution. Then, in a second test campaign, some alternative solvent systems will be studied, including the influence of additives like corrosion and degradation inhibitors.

First, the different experiments performed so far and their operating conditions will be described. Since it is an experimental work, numerous practical problems have been experienced that have slowed down the initial planning. Those experimental problems will be briefly evocated in order to get an experimental feed-back for further tests. Then, the analytical results obtained for each experiment will be presented and discussed. Those results are structured as follows:

- MEA quantification by HPLC method
- GC spectra of degraded MEA samples
- Analysis of foreign ions present in solution (metals and halogens)

4.4.1 Description of the experiments

Since the beginning of the first experiment campaign in March 2011, ten experiments have been performed to evaluate the influence of different parameters on degradation. Table 4.9 summarizes those experiments and their operating conditions.

Apart from experiments 8 and 9 which have lasted for one week, every experiment was planned to last for 2 weeks. However, two experiments had to be stopped before the end due to experimental problems that will be evocated further. For each experiment, a sample is taken from the initial amine solution and from the final solution (generally after two weeks or after one week for experiment 8 and 9). When the experiment had to be stopped before term, a sample was taken just before stopping the experiment. Those samples were conserved in a fridge until the analysis in order to stop the degradation reactions.

Table 4.9: Operating conditions of the degradation experiments

Operating conditions													
Name	Experiment Start	Experiment end	Length [Days]	Parameter tested	T [°C]	P_{tot} [bar]	P_{O2} [bar]	P_{CO2} [bar]	P_{N2} [bar]	Gas flow [mln/min]	Solvent [wt% MEA]	Mass balance [%]	Problems
Experiment 1	19/02/2011	5/03/2011	14	Base case	120	4	0.2	3	0.8	80	30.00	not recorded	-
Experiment 2	24/03/2011	5/04/2011	12	Exp. Length/strong cond.	140	20	1	15	4	200	30.00	-3.33	Gas exhaust stopped due to crystal formation in the condenser, pressure up to 25 bar
Experiment 3	11/04/2011	25/04/2011	14	Temperature	120	20	1	15	4	200	30.01	10.07	-
Experiment 4	10/05/2011	19/05/2011	9	Pressure (N_2)	140	20	0.2	3	16.8	500	30.05	-1.43	Foaming, temperature sensor defectuous => heating stopped automatically
Experiment 5	27/05/2011	10/06/2011	14	Repetability	120	4	0.2	3	0.8	80	30.01	-62.33	Crystal formation in the condenser, pressure up to 20 bar for a few hours, mass losses
Experiment 6	1/07/2011	15/07/2011	14	Repetability	120	4	0.2	3	0.8	80	30.02	-47.60	Mass losses (150g)
Experiment 7	20/07/2011	3/08/2011	14	Batch	120	20	0.2	3	0.8	0	29.99	-0.33	Corrosion of the temperature sensor
Experiment 8	24/08/2011	31/08/2011	7	Temperature and gas flow	120	20	0	0	20	20	30.00	-2.33	-
Experiment 9	31/08/2011	9/09/2011	9	Temperature and gas flow	120	20	0	0	20	200	30.00	-3.70	Gas bottle empty (2 days), current shortage
Experiment 10	13/09/2011	27/09/2011	14	New base case	120	4	0.2	0.6	3.2	160	29.99	-11.30	Mass losses

4.4.2 Experimental feed-back

Many experimental problems have been experienced during this first test campaign. Next to numerous minor problems like gas leakages, solution foaming by high gas flow, pressure oscillations… some major problems occur regularly. Those problems are briefly described in this section in order to draw a feed-back that could be helpful for further experimental works. The main problems experienced are listed below:

- **Corrosion**: the amine solvents and the degradation products are corrosive to stainless steel, included T316. The first traces of corrosion have been detected very early in the reactor vessel. A long passivation procedure has then been performed with successively distilled water and nitric acid in order to protect the metal surface from further attacks. It appears now that although the passivation was necessary, a rough passivation would have been enough and would have saved a lot of time.

  The conclusion was that corrosion cannot be prevented. It continuously takes place in the degradation reactor, but it is regularly controlled by conductivity measurement and ion analysis to be sure it doesn't dramatically increase. Since metal and halogen ions are implied in the corrosion phenomenon, their concentration in the solution is measured after each experiment so that the corrosion can be followed up.

- **Crystal formation**: The gas exiting the degradation reactor flows up into a condenser where it is cooled down, as described in section 4.2.3. The liquid condensate normally refluxes to the reactor. However, the diameter of the reflux pipe is relatively small and in some place, the liquid is stagnating, leading to crystallization of the liquid. Those crystals accumulate and finally form a plug, so that the gas cannot exit the reactor anymore. This leads to an undesired pressure increase. The first time that this problem occurred, the experiment had to be stopped before its term. Once the problem has been identified, it was possible to clean the condenser without stopping the experiment.

- **Mass balance regulation**: the regulation of the mass balance is a problem that has been reported in the literature by all research groups performing semi-batch experiments with continuous gas flow. Since gas flows through an aqueous liquid, it is saturated with water when exiting the reactor. In order to minimize the water loss, it is condensed at the reactor exit and saturated with water before flowing into the reactor. Condensation and saturation take place at the same temperature. However, the mass balance of the solution, i.e. the liquid weight difference between the experiment start and the experiment end often fluctuates (see table 4.9).

  This problem has not been solved yet. However, in order to quantify the impact of this fluctuation on the amine concentration, it has been decided to measure the water concentration of initial and final samples by Karl-Fischer titration.

- **Temperature regulation**: One experiment (experiment 4) had to be stopped before term because of a defective connection on the temperature sensor controlling the reactor temperature. This triggered the test rig emergency shut-down. The sensor was replaced by another in-house sensor, which appeared to be much more sensitive to corrosion. Finally, a new sensor was purchased. It was also necessary to repair the original heating mantle of the reactor which induced an electrical shortcut.

- **Agitation**: the agitation shaft furnished with the reactor appeared to be not perfectly straight. This implied some damages on the PTFE bushing connecting the agitator to a guide fixed to the cooling coil (see figure 4.23). As a result, Fluorine was detected during the halogen ions analysis in the amine solution. Fluorine may have been released from the PTFE bushing due to mechanical rubbing caused by the non centered rotation of the agitator.

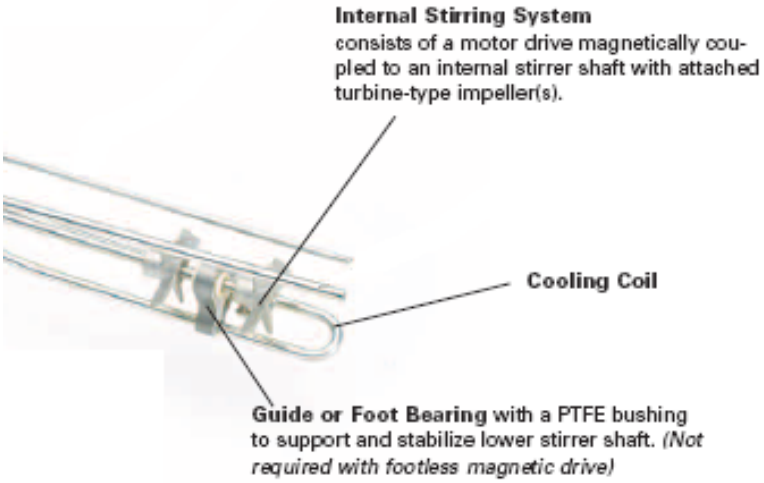

Figure 4.23: Guide with PTFE bushing for the agitator support

4.4.3 HPLC Quantification of MEA degradation

The objective of the HPLC analysis is to quantify the MEA concentration in the degraded solution at the end of the experiment. For each experiment, the final sample has been diluted 10 times with distillated water before injection.

Figure 4.24 represents the MEA concentration for each experiment. The results can be seen in table 4.10 as well. The initial concentration was always 30 wt-% MEA (see also table 4.9). The mean error value has been calculated and equals 2%.

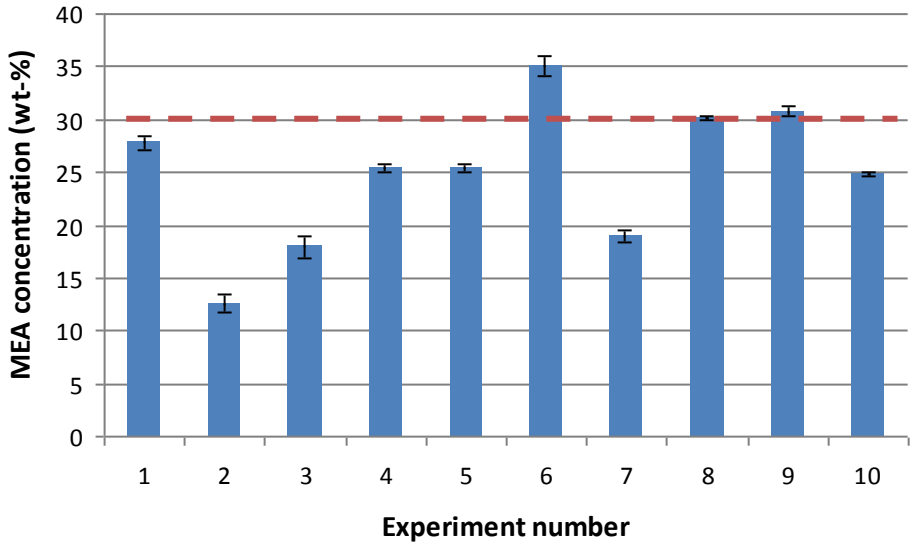

Figure 4.24: MEA concentrations measured during the degradation experiments

Table 4.10: MEA concentration at the experiments' end

Experiment	MEA concentration (wt-%)	MEA concentration change (%)
1	27.79	-7.4
2	12.57	-58.1
3	17.93	-40.2
4	25.44	-15.2
5	25.44	-15.2
6	35.07	+16.9
7	19.02	-36.6
8	30.16	+0.5
9	30,79	+2.6
10	24.80	-17.3

Those results must be considered in parallel with the mass balance data. It is the only way to explain that the MEA concentration sometimes increases: in fact, some water is evaporated and exits the reactor, so that the relative amine concentration increases, even if the total amine

amount remains unchanged. This is the case by Experiments 8 and 9: no degradation could be observed, which confirms that in the absence of O_2 and CO_2, degradation can be neglected, even at 120°C. The absence of degradation was confirmed by the GC spectra (see section 4.4.4) and the sample color, identical to non-degraded MEA. In the case of Experiment 6 however, the sample color was like degraded MEA, very dark. The high MEA concentration is clearly due in this case to the water losses. In order to solve this incertitude, the samples will be analyzed for water content using a Karl-Fisher titration. The samples have been sent for analysis and results should be available within a few weeks.

When comparing the results with the base case results (Experiment 1), some conclusions can be drawn. First, the degradation observed by the Experiment 2 is as expected the highest since the operating conditions were effectively the strongest in that case. Then, it is possible to see that the temperature has an important impact on the degradation, since the only difference between experiments 2 and 3 is that the temperature has been decreased to 120°C instead of 140°C. We can see that operating the degradation test rig in batch mode leads to high degradation rate as well.

Finally, working at high N_2 pressure low O_2 and CO_2 content does not lead to strong degradation as it can be observed from Experiment 4. Experiment 1 and 4 show approximately the same final MEA concentration. The difference could be explained by the temperature difference between both experiments.

It is important to observe that repeatability could not be achieved so far, mainly due to mass balance problems in the reactor.

4.4.4 GC spectra of degraded MEA

The final samples of Experiments 1 to 10 have been analyzed using gas chromatography. The first objective is to draw qualitative results about the degradation products contained in the samples. In a second analysis phase, those degradation products shall be quantified.

Since the degradation extent is different depending on the experiments, some samples have been diluted 10 times and other 50 times with distillated water before the injection. The chromatograms are presented in this section.

On figure 4.25, we can distinguish the MEA peak, as well as seven other degradation products. Some products can already be identified as shown in table 4.11.

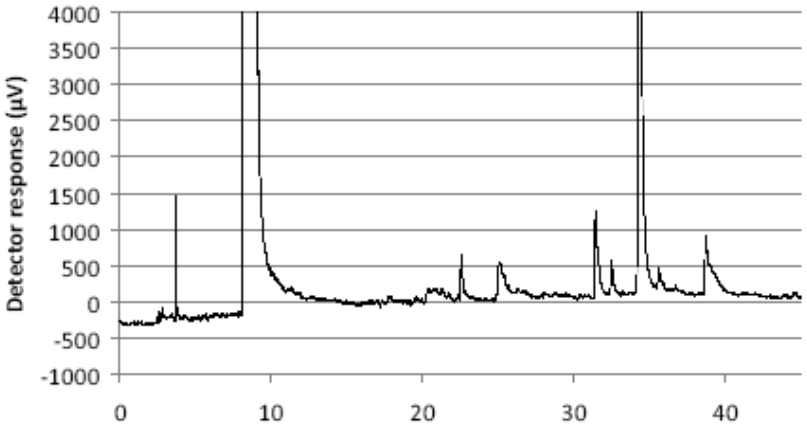

Figure 4.25: GC spectrum of Experiment 1, final sample, diluted 1:10

Table 4.11: Main degradation products in Experiment 1

Compound	Elution interval (min)	Maximum (µV)
MEA	8.17 – 10.72	156 304
OZD	22.53 – 22.74	647
HEI	24.98 – 25.59	538
HEIA	31.37 – 31.89	1259
Product 1	32.44 – 32.73	575
Product 2	34.16 – 35.29	9525
Product 3	35.53 – 36.01	457
Product 4	38.63 – 39.83	904

The same analysis can be performed for the other experiments: see Figures 4.26 to 4.34 and Tables 4.12 to 4.20

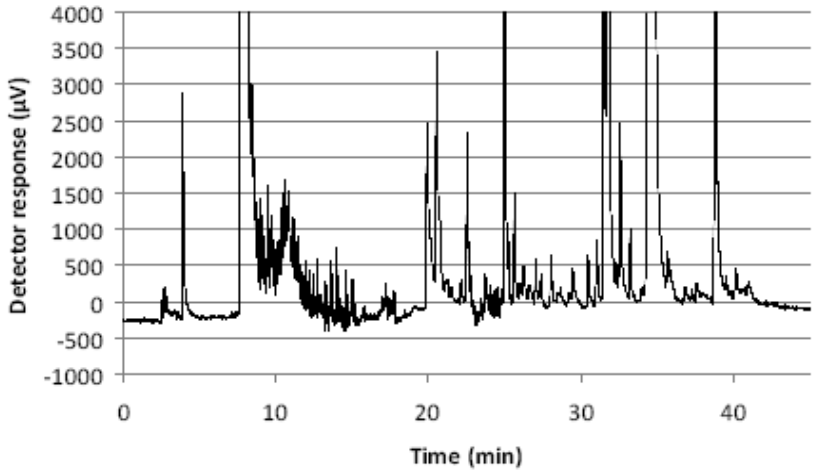

Figure 4.26: GC spectrum of Experiment 2, final sample, diluted 1:10

Table 4.12: Main degradation products in Experiment 2

Compound	Elution interval (min)	Maximum (µV)
MEA	7.56 – 8.79	87424
Acetamide	10.48 –10.9	1517
Product 5	19.84 – 20.06	2458
Product 6	20.46 – 20.76	3444
OZD	22.49 – 22.60	2329
HEI	24.92 – 25.12	5002
Product 7	25.62 – 25.68	1491
Product 8	31.42 – 31.6	7306
HEIA	31.6 – 32.00	7306
Product 1	32.52 – 32.63	2470
Product 2	34.26 – 35.19	24562
Product 3	35.62 – 36.79	685
Product 4	38.71 – 39.04	4826

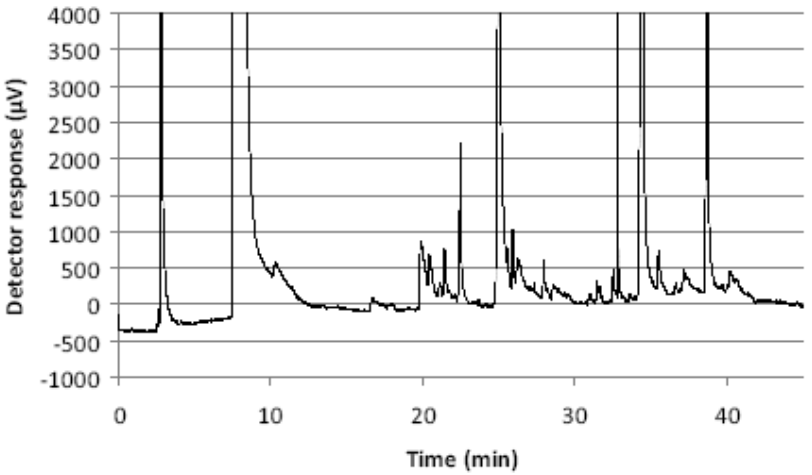

Figure 4.27: GC spectrum of Experiment 3, final sample, diluted 1:10

Table 4.13: Main degradation products in Experiment 3

Compound	Elution interval (min)	Maximum (µV)
MEA	7.42 – 8.97	93184
Acetamide	10.22 – 10.48	569
Product 5	19.80 –20.16	863
Product 6	20.40 – 20.53	674
Product 9	21.40 – 21.49	772
OZD	22.38 – 22.56	2222
HEI	24.81 – 25.64	7629
Product 10	25.87 – 26.03	1017
Product 11	26.18 – 26.43	632
Product 12	27.93 – 27.98	601
Product 2	34.18 – 34.88	10420
Product 3	35.47 – 35.60	745
Product 4	38.55 – 39.01	5631

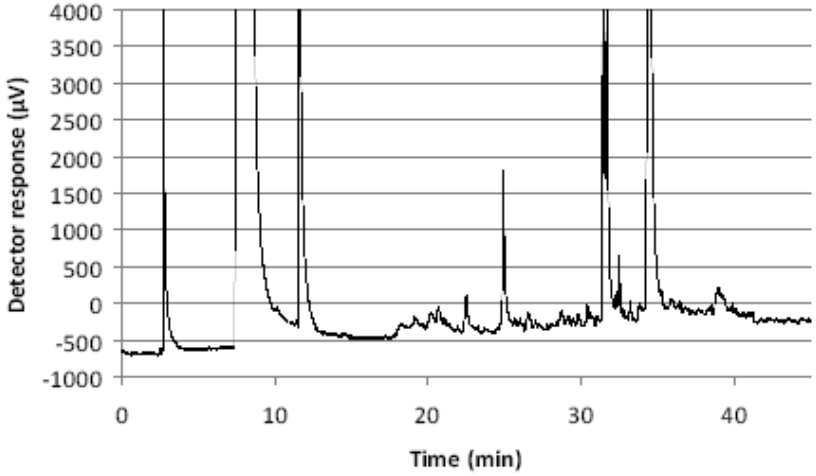

Figure 4.28: GC spectrum of Experiment 4, final sample, diluted 1:10

Table 4.14: Main degradation products in Experiment 4

Compound	Elution interval (min)	Maximum (µV)
MEA	7.38 – 9.75	96072
Product 13	11.55 – 12.22	1155312
OZD	22.40 – 22.57	103
HEI	24.84 – 25.21	1822
HEIA	31.34 – 32.18	4891
Product 1	32.18 – 32.63	638
Product 2	34.13 – 35.70	11889
Product 4	38.70 – 39.47	215

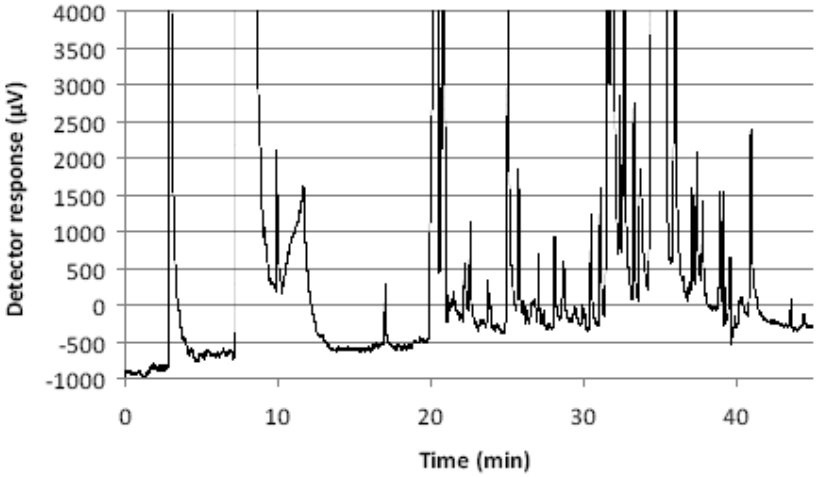

Figure 4.29: GC spectrum of Experiment 5, final sample, diluted 1:10

Table 4.15: Main degradation products in Experiment 5

Compound	Elution interval (min)	Maximum (µV)
MEA	7.24 – 9.90	155560
Product 14	9.90 – 10.31	2104
Acetamide	10.31 – 12.18	1627
HEEDA	16.94 – 17.21	281
Product 5	19.90 – 20.59	9875
Product 6	20.60 – 21.04	6306
Product 9	21.38 – 21.60	186
Product 15	22.18 – 22.40	556
OZD	22.49 – 22.69	1131
Product 16	23.72 – 23.82	329
HEI	24.96 – 25.51	5520
Product 7	25.66 – 25.92	1844
Product 12	28.07 – 28.22	933
Product 17	30.45 – 30.60	1219
Product 18	31.03 – 31.26	1594

Product 8	31.45 – 31.72	10905
HEIA	31.73 – 32.31	8017
Product 1	32.53 – 33.20	7557
Product 19	33.66 – 34.02	1850
Product 2	34.24 – 35.80	71704
Product 3	35.81 – 36.82	5689
Product 20	37.06 – 37.89	2079
Product 4	38.88 – 39.09	1536
Product 21	40,20 – 40,47	114
Product 22	40.87 – 41.34	2386

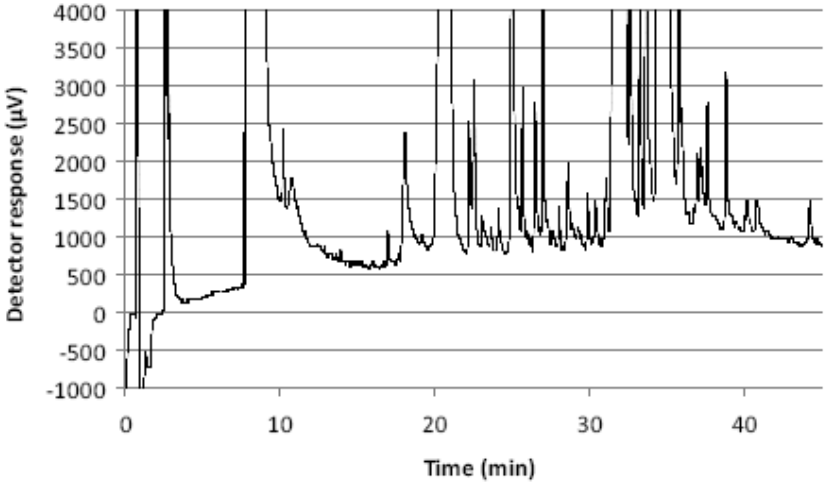

Figure 4.30: GC spectrum of Experiment 6, final sample, diluted 1:10

Table 4.16: Main degradation products in Experiment 6

Compound	Elution interval (min)	Maximum (µV)
MEA	7.82 – 10.16	171352
Product 14	10.17 – 10.39	2429
Acetamide	10.60 – 10.99	1767
HEEDA	16.96 – 17.11	1066
Product 23	17.85 – 18.74	2355
Product 5	19.94 – 20.73	10573
Product 6	20.74 – 21.11	8396
Product 15	22.16 – 22.40	2536
OZD	22.40 – 22.80	3041
Product 16	23.63 – 23.71	1116
HEI	24.83 – 25.56	11682
Product 7	25.57 – 25.90	2964
Product 24	26.90 – 27.41	4495
Product 12	28,00 – 28.11	1391
Product 18	31.03 – 31.13	1745
Product 8	31.37 – 31.71	16451
HEIA	31.72 – 32.52	17619
Product 1	32.53 – 32.90	5416
Product 19	33.55 – 34.17	8599

Product 2	34.25 – 35.29	30928
Product 3	35.69 – 36.18	4440
Product 20	37.10 – 37.40	2174
Product 4	38.75 – 38.95	3156
Product 21	40.00 – 40.34	1445
Product 22	40.72 – 40.99	1472
Product 25	44.13 – 44.43	1467

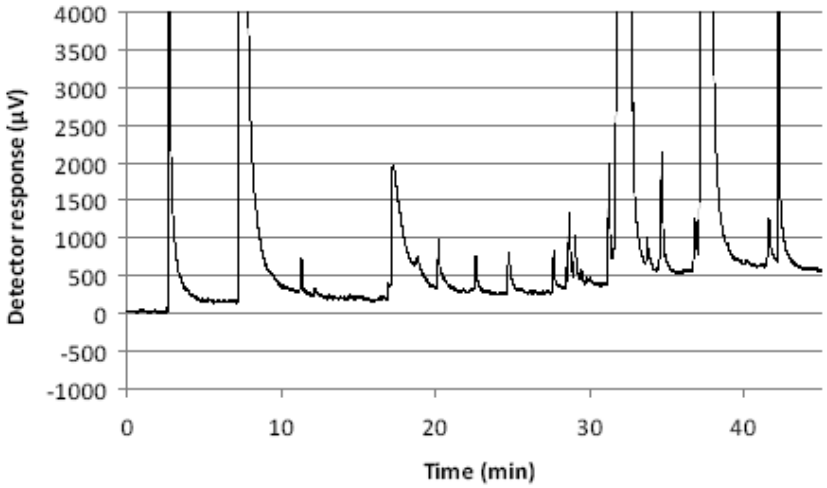

Figure 4.31: GC spectrum of Experiment 7, final sample, diluted 1:10

Table 4.17: Main degradation products in Experiment 7

Compound	Elution interval (min)	Maximum (µV)
MEA	7.27 – 9.53	121976
Acetamide ?	11.26 – 11.40	726
HEEDA	17.13 – 18.69	1956
Product 5	20.12 – 20.45	981
OZD	22.53 – 22.77	760
HEI	24.65 – 25.03	801
Product 18	31.14 – 31.42	1989
HEIA	31.57 – 32.25	32416
Product 2	34.54 – 34.85	2138
Product 20	37.04 – 37.64	22373
Product 26	37.65 – 38.97	12294
Product 27	41.52 – 41.84	1249
Product 28	42.24 – 42.79	8010

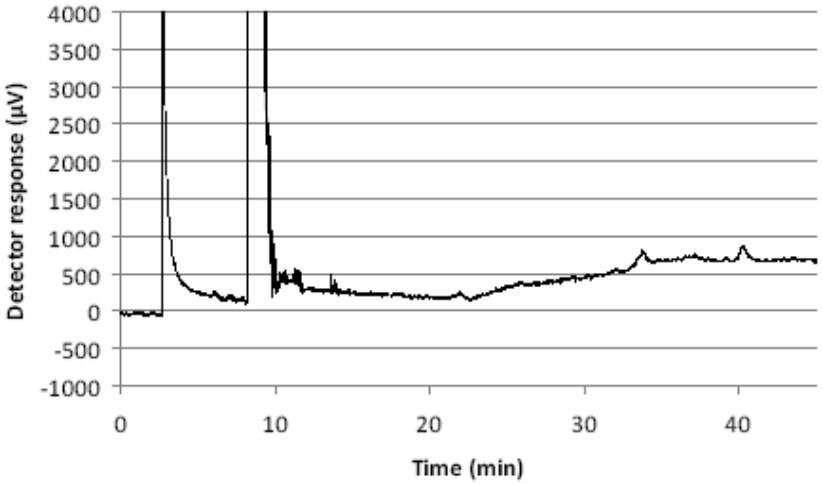

Figure 4.32: GC spectrum of Experiment 8, final sample, diluted 1:10

Table 4.18: Main degradation products in Experiment 8

Compound	Elution interval (min)	Maximum (µV)
MEA	8.18 – 9.84	173328
Product 19	33.5 – 34.06	823
Product 21	39.80 – 40.89	877

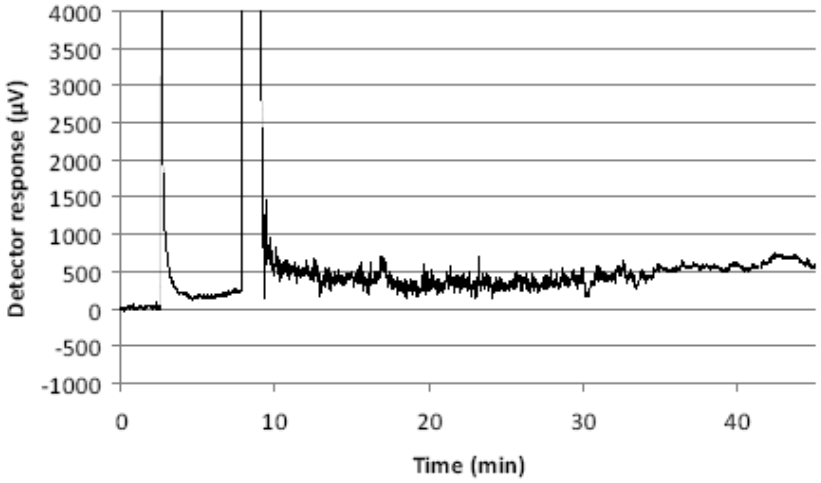

Figure 4.33: GC spectrum of Experiment 9, final sample, diluted 1:10

Table 4.19: Main degradation products in Experiment 9

Compound	Elution interval (min)	Maximum (µV)
MEA	7.83 – 9.27	433168
HEA?	16.88 – 19.25	691

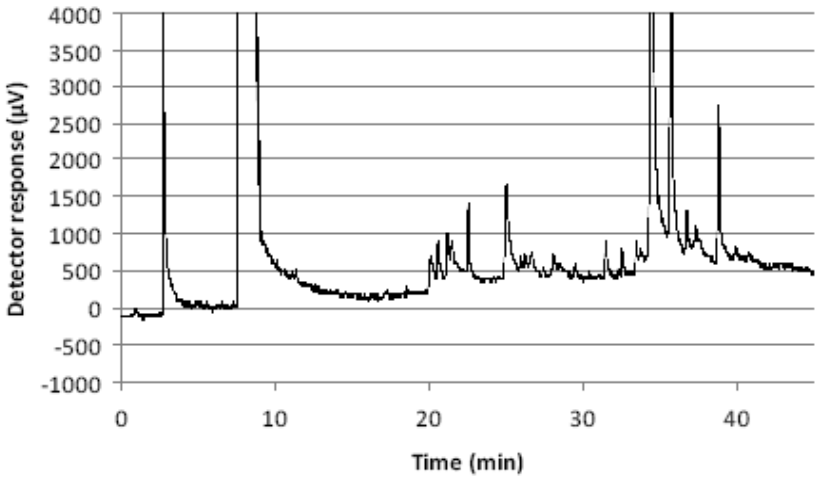

Figure 4.34 : GC spectrum of Experiment 10, final sample, diluted 1:10

Table 4.20: Main degradation products in Experiment 10

Compound	Elution interval (min)	Maximum (µV)
MEA	7.57 – 9.51	150816
Product 5	20.02 – 20.30	678
Product 6	20.53 – 20.80	888
Product 29	21.09 – 21.37	1024
Product 9	21.38 – 22.24	926
OZD	22.46 – 22.78	1396
HEI	24.90 – 25.88	1668
HEIA	31.44 – 31.76	914
Product 1	32.49 – 32.77	803
Product 2	34.26 – 35.51	9946
Product 3	35.52 – 36.22	4830
Product 20	37.13 – 37.79	1128
Product 4	38.73 – 39.33	2719

Table 4.21 summarizes the previous results. Most of the unknown products that appear only once in the previous spectra may be due to contaminations, or detection errors. However, many of those products appear regularly, as it can be observed in Table 4.21. It could be interesting to identify those products for a better understanding of the degradation phenomena.

Table 4.21: Degradation products in each experiment

Experiment Product	1	2	3	4	5	6	7	8	9	10
MEA	x	x	x	x	x	x	x	x	x	x
Acetamide		x	x		x	x	x			
HEEDA					x	x	x			
HEA									x	
OZD	x	x	x	x	x	x	x			x
HEI	x	x	x	x	x	x	x			x

HEIA	x	x		x	x	x	x		
Product 1	x	x		x	x	x			x
Product 2	x	x	x	x	x	x	x		x
Product 3	x		x		x	x			x
Product 4	x		x	x	x	x			x
Product 5		x	x		x	x	x		x
Product 6		x	x		x	x			x
Product 7		x			x	x			
Product 8		x			x	x			x
Product 9			x		x				x
Product 10			x						
Product 11			x						
Product 12			x		x	x			
Product 13				x					
Product 14					x	x			
Product 15					x	x			
Product 16					x	x			
Product 17					x				
Product 18					x	x	x		
Product 19					x	x		x	
Product 20					x	x	x		x
Product 21					x	x		x	
Product 22					x	x			
Product 23						x			
Product 24						x			
Product 25						x			
Product 26							x		
Product 27							x		
Product 28							x		
Product 29									x

4.4.5 Ion analysis results

In order to follow the corrosion phenomena that take place inside the degradation reactor, it has been decided to measure the quantity of some particular metal and halogen ions that play a role in corrosion. After each degradation experiment, samples are sent to the Laboratory for Hydrogeology of the University of Liège where the samples are analyzed. Table 4.22 presents the evolution of ions in solution.

Table 4.22: Evolution of ion concentrations in solution, in ppm

	Fe	Cr	Ni	Si	Cl	F
MEA 30%	0.44	< 0.10	< 0.10	-[a]	< 2.00	38.944
Experiment 1	7.57	1.55	4.24	-[a]	< 2.00	416.08
Experiment 2	22.40	8.60	9.75	13.01	513.16	1826.18
Experiment 3	6.80	3.10	2.66	10.66	522.32	869.35

Experiment 4	1.90	1.30	1.01	15.57	291.36	307.13
Experiment 6[b]	14,70	2.75	159	2754.21	< 5.00	594.62
Experiment 7	66.10	7.50	571	147.78	< 5.00	321.14
Experiment 8	0.19	2.27	0.69	94.80	< 5.00	251.55
Experiment 9	0.14	2.39	0.51	95.55	< 5.00	276.30
Experiment 10	3.46	6.41	0.87	557.55	29.34	532.38

[a] Silicon has not been measured for the two first samples

[b] Final sample from Experiment 5 still has to be analyzed

Iron, Chromium, and Nickel concentrations are most of the time really well correlated. These three metals are present in T316 stainless steel. When their concentration is high, it means that the reactor has been damaged by the amine solution and that a lot of those ions dissolved in the liquid phase. Based on this assumption, it is possible to conclude that some degradation products presents in Experiments 2, 6 and 7 are very corrosive.

What concerns the concentration of Chlorine and Fluorine, they are not related to the metal ions concentrations (see Experiment 4 for instance). However, it is known that Chlorine and Fluorine are very corrosive elements. We can conclude from this that Chlorine and Fluorine are not influencing the corrosion of the degradation vessel. However, their presence and the way they vary remain unexplainable, especially for Chlorine since the presence of Fluorine could be explained by the problems related to the agitator described in section 4.4.2. The presence of Silicon remains unexplainable as well. One possible hypothesis is that some Silicon may come from lubricant used in the magnetic agitation system of the reactor. However, it is possible to deduce from the results presented here that Silicon has no influence on corrosion either.

The follow-up of corrosion will continue during the next experiments. Moreover, a detailed inspection of the reactor vessel by corrosion experts from Laborelec is planned to be sure that corrosion remains under control.

4.4.6 Karl-Fischer titration results

The results obtained by the Karl-Fischer titration are presented in table 4.23. The objective is to correlate them with the mass losses results recorded during the degradation experiments. Consequently, the relative amount of evaporated water during the experiment can be determined and the mass balance can be checked. Figure

Table 4.23: Results of the KF analysis and comparison with mass balance results

Experiment	Water balance	Mass balance
Experiment 1	-9%	Not recorded
Experiment 2	2%	-3%
Experiment 3	-3%	+10%
Experiment 4	-3%	-1%
Experiment 5	-36%	-62%
Experiment 6	-49%	-48%
Experiment 7	0%	0%
Experiment 8	-1%	-2%
Experiment 9	-4%	-4%
Experiment 10	-8%	-11%

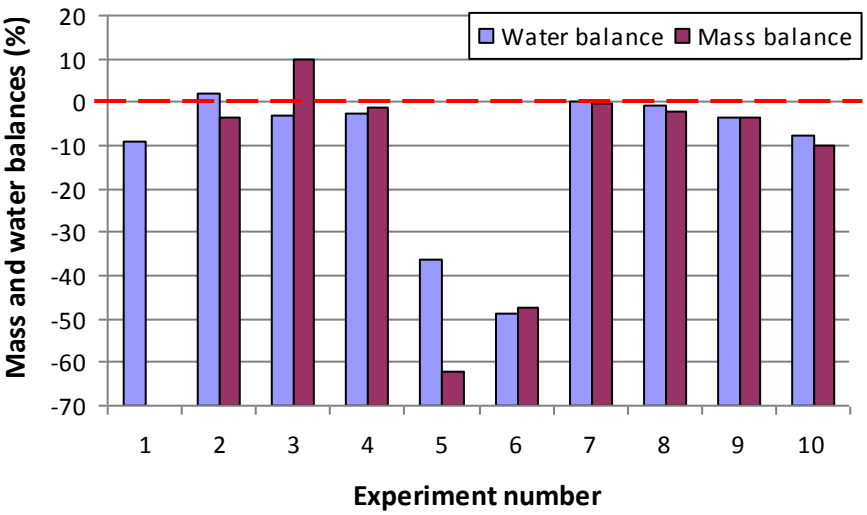

Figure 4.35: Results of the KF analysis and comparison with mass balance results

We can see that both results are quite well correlated, which means that mass losses and water losses vary during degradation experiments in the same proportions.

5 Conclusion and perspectives

The present report describes the work that has been performed the last two years in the framework of a PhD thesis at the University of Liège. This work results from a collaboration between the company Laborelec and the University of Liège. The application fields of this thesis are divided into two main parts.

First, the simulation of the post-combustion CO_2 capture process in a coal-fired power installation with monoethanolamine is studied using two different models. The first model makes some equilibrium assumptions regarding the mass transfer columns and neglects geometry and kinetics parameters. The second model takes those parameters into account. For each model, the simulation has been performed in two steps. The first step consisted in the identification and the sensitivity study of process parameters having a large influence on the capture energetic efficiency. The second step consisted in the implementation of process modification with the same goal of reducing the energy requirement of the CO_2 capture. Those studies have shown that it was possible to save about 20% of the solvent regeneration energy while performing those modifications. However, the model still has to be validated to be completely reliable. Experimental data for validation purpose shall be obtained from the mobile pilot capture installation actually located in Gelderland and for which Laborelec takes part to the development.

The second objective is to perform an experimental study of solvent degradation in the case of CCS solvents. Since the cost related to solvent replacement reaches approximately 22% of the OPEX (Abu Zahra, 2009), it is essential to consider solvent degradation prior to any scale-up operation. In this optic, a test rig has been built at the University of Liège to assess the degradation of solvents under accelerated degradation conditions. This equipment allows for batch and semi-batch studies, in which a gas mix is continuously bubbling through the solvent solution. High pressure and high temperature conditions may be imposed in order to accelerate the degradation phenomena. The results of the first test campaign are presented in this report. Different analytical means have been developed to assess precisely the solvent degradation in the liquid phase, as well as in the gas phase. The development of those methods is still under progress, but good results have been recorded, especially using Gas Chromatography and High Performance Liquid Chromatography. Many experimental problems have been met and solved, so that the second test campaign may allow a complete characterization of monoethanolamine degradation. Perspectives regarding degradation studies also include the test of additives such as degradation inhibitors.

Finally, the main objective of the PhD thesis is to develop a validated simulation model including degradation data. Based on this model, it will be possible to perform a multi-objective optimization of the CO_2 capture process, considering the influence of key process parameters on regeneration energy requirement as well as on degradation extent. Based on a cost approach, this multi-objective optimization should lead to a proposition for optimal operating conditions regarding energy efficiency as well as degradation and environmental performance.

6 Bibliography

Abu Zahra M., **2009**, Carbon dioxide capture from flue gas, PhD Thesis at Delft University, Netherlands

Aspen Tech, **2011**, Apr System Help, Electrolyte NRTL, Development of the Model

Bedell S., **2009**, Oxidative degradation mechanisms for amine in flue gas capture, Energy Procedia 1 (2009) 771–778

Bello A. and Idem R., **2005**, Pathways for the Formation of Products of the Oxidative Degradation of CO2-Loaded Concentrated Aqueous Monoethanolamine Solutions during CO2 Absorption from Flue Gases, *Ind. Eng. Chem. Res.* 2005**,** *44,* 945-969

Bello A. and Idem R., **2006**, Comprehensive Study of the Kinetics of the Oxidative Degradation of CO2 Loaded and Concentrated Aqueous Monoethanolamine (MEA) with and without Sodium Metavanadate during CO2 Absorption from Flue Gases, *Ind. Eng. Chem. Res.* 2006, *45,* 2569-2579

Bacot S., Picq D., Carrette P-L., Kittel J., **2007**, Nouvelles amines permettant le captage du CO_2 : dégradation et corrosivité, projet CapCO_2, Présentation réalisée à Pau,12 et 13 décembre 2007

Captech, **2008**, Advanced Solvent Development at Shell, 2nd CAPTECH Day, Arnhem, 06. March 2008

Chi S., Rochelle, G., **2001**, Master Thesis, Oxidative Degradation of Monoethanolamine, University of Texas at Austin, USA

Davis J., **2009**, Thermal Degradation of Aqueous Amines Used for Carbon Dioxide Capture, PhD Thesis, University of Texas at Austin, USA

Davis J., Rochelle, G., **2009,** Thermal degradation of monoethanolamine at stripper conditions, Energy Procedia 1, 2009 327-333

Dubois L., Thomas D., **2009,** CO_2 Absorption into Aqueous Solutions of Monoethanolamine, Methyldiethanolamine, Piperazine and their Blends, Chem. Eng. Technol. 2009, 32, No. 5, 1–10

Goff and Rochelle, **2004**, Monoethanolamine Degradation: O_2 Mass Transfer Effects under CO2 Capture Conditions, *Ind. Eng. Chem. Res.* 2004**,** *43,* 6400-6408

Goff, **2005**, Oxidative degradation of aqueous MEA in CO_2-capture processes: Iron and copper catalysis, Inhibition and O_2 mass transfer, PhD Thesis, University of Texas at Austin, USA

Goff and Rochelle, **2006**, Oxidation Inhibitors for Copper and Iron Catalyzed Degradation of Monoethanolamine in CO_2 Capture Processes, *Ind. Eng. Chem. Res.* 2006, *45,* 2513-2521

IPCC, **2005**, IPCC special report on carbon dioxide capture and storage, Cambridge university press

Kaminski, M.; Jastrzebski, D.; Przyjazny, A.; Kartanowicz, R., **2002**, Determination of the Amount of Wash Amines and Ammonium Ion in Desulfurization Products of Process Gases and Results of Related Studies, *J. Chromatogr. A* 2002, *947*, 217.

Knudsen J., Jensen J., Vilhelmsen P., Biede O., **2007,** First year operation experience with a 1 t/h CO2 absorption pilot plant at Esbjerg coal-fired power plant Proceedings of European Congress of Chemical Engineering (ECCE-6) Copenhagen, 16-20 September 2007

Knudsen J., Vilhelmsen P., Jensen J., Biede O., **2009**, Experience with CO_2 capture from coal flue gas in pilot scale, Energy proceedia 1, 2009, 783-790.

Lawal A. and Idem R., **2005**, Effects of Operating Variables on the Product Distribution and Reaction Pathways in the Oxidative Degradation of CO2- Loaded Aqueous MEA-MDEA Blends during CO2 Absorption from Flue Gas Streams, *Ind. Eng. Chem. Res.* 2005, *44*, 986-1003

Lawal A., Bello A. and Idem R., **2005**, The Role of Methyl Diethanolamine (MDEA) in Preventing the Oxidative Degradation of CO2 Loaded and Concentrated Aqueous Monoethanolamine (MEA)-MDEA Blends during CO2 Absorption from Flue Gases, *Ind. Eng. Chem. Res.* 2005, *44*, 1874-1896

Lawal A. and Idem R., **2006**, Kinetics of the Oxidative Degradation of CO2 Loaded and Concentrated Aqueous MEA-MDEA Blends during CO2 Absorption from Flue Gas Streams, *Ind. Eng. Chem. Res.* 2006, *45*, 2601-2607

Lawal A., Wang M., Stephenson P., Yeung H., **2008**, Dynamic modelling of CO_2 absorption for post combustion capture in coal-fired power plants, Fuel, doi:10.1016/j.fuel.2008.11.009

Léonard G., **2009**, Modeling of a pilot plant for the CO_2-reactive absorption in amine solvent for power plant flue gases, Master Thesis at University of Liège, Belgium

Lepaumier H., **2008**, Etude des mécanismes de dégradation des amines utilisées pour le captage du CO_2 dans les fumées, PhD thesis at the University of Savoie, France

Lepaumier H., Picq D., Carrette P., **2009**, Degradation Study of new solvents for CO_2 capture in post combustion, Energy Procedia 1, 2009, 893-900

Lepaumier H., da Silva E., Einbu A., Grimstvedt A., Knudsen J., Zahlsen K., Svendsen H., **2010**, Comparison of MEA degradation in pilot-scale with lab-scale experiments, Energy Procedia 4, 2011, 1652‑1659

Notz R., Asprion N., Clausen I. and Hasse H., **2007**, Selection and pilot plant tests of new absorbents for post-combustion carbon dioxide capture, doi: 10.1205/cherd06085

Notz R., **2009**, CO2-Abtrennung aus Kraftwerksabgasen mittels Reaktivabsorption, PhD Thesis at the University of Stuttgart, Germany

Sexton A., **2008**, Amine oxidation in CO_2 capture processes, PhD Thesis at the University of Texas at Austin, Texas, USA.

Sexton and Rochelle, **2009**, Catalysts and Inhibitors for MEA Oxidation, Energy Procedia 1, 2009, 1179–1185

Supap T., Idem R., Veawab A., Aroonwilas A., Tontiwachwuthikul P., Chakma A., Kybett B., **2001**, Kinetics of the Oxidative Degradation of Aqueous Monoethanolamine in a Flue Gas Treating Unit, *Ind. Eng. Chem. Res.* 2001, *40*, 3445-3450

Supap T., Idem R., Tontiwachwuthikul P. and Saiwan C., **2006**, Analysis of Monoethanolamine and its Oxidative Degradation Products during CO_2 Absorption from Flue Gases: A Comparative Study of GC-MS, HPLC-RID, and CE-DAD Analytical Techniques and Possible Optimum Combinations, *Ind. Eng. Chem. Res.* 2006, *45*, 2437-2451

Supap T., Idem R., Tontiwachwuthikul P. and Saiwan C., **2009**, Kinetics of sulfur dioxide- and oxygen-induced degradation of aqueous Monoethanolamine solution during CO_2 absorption from power plant flue gas streams, International Journal of greenhouse gas control 3, 2009, 133–142

Uyanga I. and Idem R., **2007**, Studies of SO_2- and O_2-Induced Degradation of Aqueous MEA during CO_2 Capture from Power Plant Flue Gas Streams, *Ind. Eng. Chem. Res.* 2007, *46*, 2558-2566

Zhang Y., Chen H., Chen C.-C., Plaza J., Dugas R., Rochelle G., **2009**, Rate-based process modeling of CO_2 capture with aqueous monoethanolamine solution, Ind. Eng. Chem. Res., 48, 9233–9246

7 Abbreviation List

EDA	Ethylenediamine
FID	Flame Ionization Detector
FTIR	Fourier Transform Infra Red analysis
GC	Gas Chromatography
HEA	N-acetylethanolamine
HEEDA	2-(2-Aminoethylamino)ethanol
HEI	1-(2-Hydroxyethylimidazole)
HEIA	1-(2-Hydroxyethyl)-2-imidazolidinone
HPLC	High Performance Liquid Chromatography
IC	Intercooling
KF	Karl Fischer
LVC	Lean Vapor Compression
MEA	Monoethanolamine
OZD	Oxazolidone
PTFE	Polytetrafluoroethylene (Teflon®)
RID	Refractive Index Detector

8 Appendices

8.1 Risk analysis for the Degradation Test Rig.

This section describes in French the risk analysis that has been performed for the degradation test rig.

8.1.1 Les locaux et zones de travail

Le banc de dégradation des solvants CCS construit dans le cadre de la thèse de doctorat de G. Léonard en collaboration avec l'entreprise Laborelec se situe à la Halle de Chimie Appliquée (figure 1) à l'adresse suivante :

Halle de Chimie Appliquée,
B17, P35, Grande traverse
4000 Liège Sart-Tilman.
Tel. : 04/366 44 62

L'accès à la Halle se fait par une porte sur laquelle un affichage indique clairement que l'accès est réservé aux seules personnes autorisées ou accompagnées. En dehors des heures d'ouvertures, cette porte est fermée à clé et une alarme est activée à l'intérieur du bâtiment.

Fig. 1 : B17, Halle de chimie appliquée

Fig. 2 : Porte d'accès à la Halle

Les activités de la halle concernent le génie chimique et génie des procédés. Les principales activités sont les suivantes : études hydrodynamiques de cuves agitées et de colonnes à empilage, tomographie rayons X, isothermes d'adsorption de polluants, séchage de boues d'épuration, …

Le réacteur de dégradation se situe à l'intérieur d'un local ventilé fermé, lui-même à l'intérieur d'une pièce ouverte sur la Halle (voir plan ci-dessous, figure 3). Il y a 2 entrées / sorties à la Halle, et les flèches rouges sur la figure 3 symbolisent les voies d'évacuation du bâtiment.

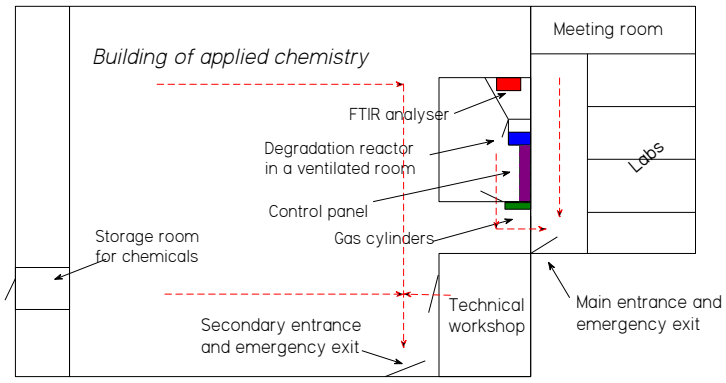

Fig. 3 : Plan de la halle de chimie appliquée

8.1.2 L'organisation technique entre postes de travail

L'installation de dégradation est composée de quatre parties principales (figures 4 à 7) :

- un local ventilé où se trouvent le réacteur et ses auxiliaires (figure 4)
- dans un deuxième local ventilé voisin de celui où se trouve le réacteur : l'analyseur FTIR (figure 5)
- à côté du local ventilé où se trouve le réacteur : le poste de contrôle, l'analyseur HPLC et les lignes d'arrivée du gaz (figure 6)
- à l'entrée de la pièce ouverte, côté Halle : les bouteilles de gaz et leur centrale de détente (figure 7).

Fig. 4 : local ventilé

Fig. 5 : Analyseur FTIR

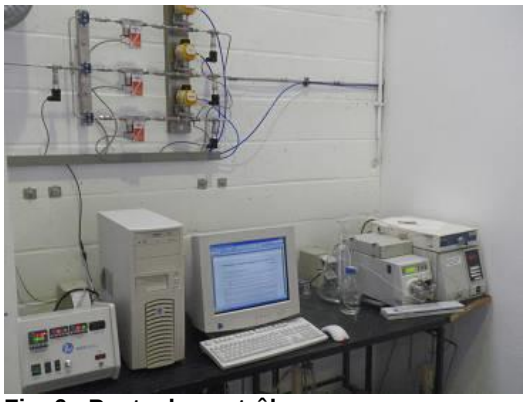

Fig. 6 : Poste de contrôle

Fig. 7 : Rack à bouteilles

Le local ventilé où se situe le réacteur de dégradation peut accueillir une personne qui manipule l'installation. Ce local doit être fermé durant les manipulations entre les expériences ainsi que lors des expériences.

La pièce dans laquelle se situe ce local ventilé est partagée entre deux utilisateurs réguliers. Le premier utilisateur régulier travaille sur l'installation située dans le même local ventilé que l'analyseur FTIR. Le deuxième utilisateur régulier est l'opérateur du banc de dégradation. Occasionnellement, d'autres utilisateurs pénètrent dans cette pièce pour avoir accès aux machines qui s'y trouvent (étuve, centrifugeuse).

Cette pièce a une seule porte d'accès, tout comme le local ventilé. Les voies de circulation dans la pièce sont clairement délimitées. L'accès aux zones de travail se fait sans problème. L'encombrement devra être limité au strict nécessaire, et des rangements réguliers (une fois tous les mois au minimum) seront prévus pour éviter l'accumulation de matériel dans les locaux et zones de travail.

8.1.3 Prévention des accidents de travail

Les équipements de protection individuelle nécessaires sont disponibles à la halle : tabliers de laboratoires, lunettes de protection, gants adaptés à la manipulation de solutions aminées.

Ils se trouvent dans une armoire située à côté de la porte d'entrée de la pièce ouverte sur la Halle (figure 8). Dans cette armoire se trouve également un flacon de produit nettoyant pour rincer les yeux en cas de contact avec un produit non désirable. La durée de validité de ce produit est contrôlée régulièrement.

Fig. 8 : Equipements de protection individuelle

La boite de premiers soins se trouve près des toilettes, à côté de la salle de réunion.

La procédure à appliquer en cas d'accident est celle applicable de manière générale dans les laboratoires de l'ULg. Cette procédure est à suivre en cas d'urgence lors d'un fonctionnement défectueux de l'installation de dégradation et dans le cas où les alarmes automatiques ne se

seraient pas déclenchées. Cette procédure se trouve en première page de la farde accompagnant l'installation et qui se trouve près du panneau de contrôle.
Le fonctionnement défectueux du banc d'essai est constaté lorsque :

- une fuite importante de gaz ou de liquide audible ou observable par le hublot fixé sur la porte du local ventilé ou sur la ligne de gaz en dehors du local ventilé permet de conclure que l'installation n'est pas dans un mode de fonctionnement habituel ou prévu par l'opérateur, entraînant l'apparition d'un danger potentiel pour le personnel ou le matériel à proximité.
- Une valeur anormale d'un capteur de température ou de pression est constatée, entraînant l'apparition d'un danger potentiel pour le personnel ou le matériel à proximité.
- Un bruit anormal lié à l'installation permet de conclure que l'installation n'est pas dans un mode de fonctionnement habituel ou prévu par l'opérateur, entraînant l'apparition d'un danger potentiel pour le personnel ou le matériel à proximité.
- tout autre élément significatif amenant à cette même conclusion.

La procédure à suivre en cas d'urgence est dès lors la suivante :

1. Arrêt immédiat de l'installation au moyen du bouton d'arrêt d'urgence situé sur la cloison extérieure du local ventilé
2. Arrêt du chauffage du réacteur sur le poste de contrôle situé juste à coté du local ventilé.
3. Fermeture manuelle des vannes de sécurité commandant l'arrivée de gaz au niveau des détendeurs
4. Fermeture manuelle des vannes sur les bouteilles de gaz
5. Si quelqu'un est présent dans le local ventilé où se trouve le réacteur, évacuer ce local en refermant bien la porte
6. Si la ventilation du local ventilé n'est pas activée, mise en route de la ventilation au moyen de l'interrupteur situé sur la cloison extérieure de ce local
7. En cas de danger persistant, évacuer le bâtiment en s'assurant que tout le personnel présent à l'intérieur de la halle est évacué
8. Contacter le service d'urgence au 100 (Service médical d'urgence et pompiers) ou au 112 (numéro d'appel européen en cas d'accident ou d'agression)
9. Contacter le Central d'alarme de l'ULg au numéro 04/366 44 44 (44 44 si appel interne)
10. Contacter le personnel responsable de l'installation au numéro suivant : 04/366 95 92 ou 0487/47 11 35 (GSM Grégoire Léonard).

8.1.4 Les risques électriques

L'installation électrique a été effectuée par le personnel qualifié en suivant les normes en vigueur. Différentes protections ont été prévues pour limiter les conséquences de tout dysfonctionnement électrique. Entre autres :

- un différentiel 30mA protège l'installation et ses utilisateurs en coupant l'alimentation lorsque des courants de fuite sont détectés,
- un fusible coupe le courant en cas de court-circuit ou de surintensité du courant à l'installation
- une prise de terre est établie selon les normes en vigueur et toute l'installation y est électriquement reliée.

L'appareillage électrique se situe dans un coffret facile d'accès à l'intérieur du local ventilé (figure 9). Ce coffret est fermé à clef, mais la clef est facilement accessible en cas de besoin. Un bloc mural de quatre prises électriques est également disponible dans le local ventilé en dessous du coffret électrique. Il convient de prendre garde à ne pas renverser de liquide sur le bloc ou le coffret. Pour limiter ce risque, ces deux éléments ont été placés plus haut que le plan de travail.

Le bouton d'arrêt d'urgence dont il a déjà été question est directement relié au coffret électrique et permet d'en couper l'alimentation simplement et rapidement, sans pour autant couper l'aération du local ventilé qui n'est pas branchée sur le même coffret. Un interrupteur supplémentaire avec voyant lumineux se situe sur la porte du coffret. Ce voyant étant visible à travers le hublot de la porte (figure 10), il est possible de déterminer si l'installation est sous tension ou non sans devoir pénétrer dans le local ventilé.

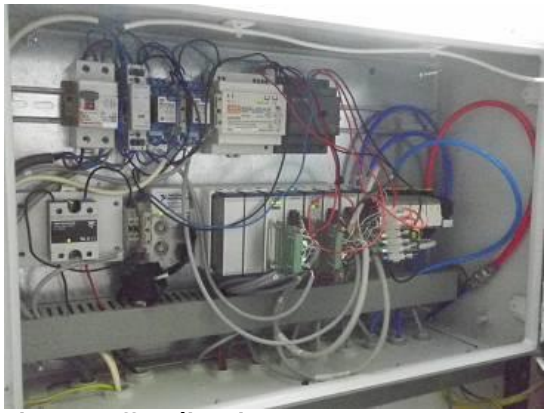

Fig. 9 : Coffret électrique

Fig. 10 : vue du coffret à travers le hublot

8.1.5 Les risques liés au gaz

Quatre bonbonnes de gaz sont fixées au mur extérieur de la pièce où se trouve le local ventilé. Il s'agit de bouteilles d'air comprimé, d'azote, de dioxyde de carbone et d'oxygène. Les fiches de sécurité relatives à ces gaz sont disponibles dans la farde accompagnant l'installation. Grâce à une identification appropriée (code couleur et plaque signalisatrice), un simple coup d'œil permet de savoir directement quel gaz est contenu dans chacune des bonbonnes. Cette même signalisation est clairement repérable sur chacune des lignes de gaz partant des bonbonnes. De plus, un affichage au-dessus des bouteilles signale les risques liés au gaz de manière explicite (figure 11). Le code couleur est repris dans le tableau ci-dessous et se trouve également dans la farde de l'installation:

Couleur	Gaz
Noir	N_2
Gris	CO_2
Blanc	O_2
Vert	Air comprimé

Les gaz sont stockés sous forme gazeuse à 200 bars sauf le CO2 qui est sous forme bi-phasique à 50 bars. Les bouteilles sont attachées par des chaînes à une armature métallique (rack) fixée au mur. Une chaîne supplémentaire retenant toutes les bouteilles est sécurisée par un cadenas (figure 12). Les bouteilles se situent à proximité de zones de passage de piétons uniquement, il n'y a pas de risque de passage de transpalette à cet endroit.

Fig. 11 : Affichage du rack à bouteilles

Fig. 12 : Chaîne de sécurité et cadenas

Le transport des bonbonnes se fait avec toutes les précautions d'usage : le capuchon de protection de la valve doit être fixé pour protéger la valve en cas de chute de la bonbonne, le déplacement se fait au moyen d'un diable conçu spécialement pour le transport de bouteilles. Les précautions à appliquer concernant la manipulation des bouteilles de gaz comprimé sont reprises à la fiche 28 p125 de la brochure sur la gestion des risques professionnels (stratégie Sobane) qui se trouve dans la farde de l'installation.

Le cas de fuites de gaz doit être également envisagé. Aucun détecteur n'est prévu car les volumes contenus dans les bouteilles sont faibles et la halle de chimie appliquée est d'un volume assez grand et continuellement aéré, ce qui limite le risque d'accumulation locale de gaz en cas de fuite importante d'un gaz. Les risques d'asphyxie sont très réduits car le volume total de gaz asphyxiant est de 27m³ (bouteilles de N_2 et CO_2) et que le volume de la halle est d'approximativement 3400m³.

Les fuites d'oxygène ne présentent pas non plus un risque exagéré car aucun élément susceptible de déclencher une étincelle ou d'enflammer le gaz de fuite ne se trouve à proximité immédiate des bonbonnes. Les bouteilles sont éloignées de toute source de chaleur. La température maximale ne doit pas dépasser les 50°C, valeur qui n'est jamais atteinte dans la halle, même en été. De plus, le volume d'oxygène qui serait ajouté à l'atmosphère de la halle en cas de fuite de tout l'oxygène présent de la bouteille ne modifierait la concentration en oxygène de la halle que de 0,3%, n'augmentant pas significativement le risque d'explosion du bâtiment.

Fig. 13 : Centrale de détente

La détente des gaz se fait au moyen de centrales de détentes constituée d'une vanne d'arrivée, d'un détendeur, d'une vanne de purge, d'une soupape de sécurité ainsi que d'une vanne de sécurité (figure 13). L'échappement des soupapes de sécurité n'est pas canalisé car la probabilité que ces soupapes soient appelées à fonctionner est très faible. De plus, si une fuite par ces soupapes survenait, celle-ci n'entraînerait pas de danger excessif au vu du paragraphe précédent. Dans le cas de la bouteille d'oxygène, la clé permettant la fixation de la bouteille à la centrale de détente a été enlevée afin d'éviter tout manipulation non autorisée.

azote

La procédure en cas d'urgence en cas de fuite importante de gaz dans le local ventilé a été décrite au point 3. En cas de fuite de gaz en dehors du local ventilé, la procédure d'arrêt d'urgence est identique. En fonction de l'endroit de la fuite, l'ordre des points peut varier.

D'autres protections programmées dans le logiciel de commande renforcent encore la sécurité. Ainsi, la pression sur les lignes de gaz est mesurée en plusieurs endroits et directement communiquée à l'ordinateur qui actionne l'arrêt d'urgence de l'installation en cas de fonctionnement en dehors des limites de sécurité prescrites par l'opérateur. Des dispositifs de purge et de relâchement manuel et/ou automatique de pression sont prévus partout où cela pourrait s'avérer nécessaire :

- soupape de sécurité et vanne de purge sur chacun des détendeurs
- soupape de sécurité et vanne de purge sur l'humidificateur de gaz
- disque de rupture sur le réacteur
- déverseur régulant la pression maximale du réacteur et évacuant le trop-plein de pression vers le conduit d'évacuation des gaz
- soupape de sécurité sur la ligne de gaz en aval du réacteur en protection de l'analyseur FTIR

Avant la mise en service de l'installation, les lignes de gaz sont contrôlées sous pression afin de repérer d'éventuelles fuites. Egalement avant la mise en service, les différents éléments de l'installation (réacteur et humidificateur de gaz) sont éprouvés sous haute pression (30bar) pour s'assurer de leur bonne tenue en cas de dépassement de la pression de consigne (fixée à 25bar au maximum). Ce contrôle pourra être renouvelé tous les ans si le besoin le justifie. Les épreuves sous pression sont décrites dans des fichiers qui seront joints à la présente analyse dès que les tests auront été effectués.

8.1.6 Les risques incendie et explosion

Les risques d'incendie et d'explosion ont déjà été partiellement abordés aux points 3 et 5. Aucune source de feu ne se trouve directement à proximité des bouteilles. Les risques d'inflammabilité de l'oxygène sont réduits par un nettoyage préalable à l'acétone des conduites et éléments en contact avec l'oxygène. En cas d'incendie dans les bâtiments, la procédure d'arrêt d'urgence de l'installation est celle qui a été décrite au point 3. Un extincteur est disponible dans le couloir d'entrée de la halle, à proximité immédiate de l'installation. La lance incendie la plus proche se trouve dans l'atelier des techniciens et a une longueur suffisante pour atteindre l'installation de dégradation et ses auxiliaires.

En cas de surpression dans le réacteur de dégradation ou sur les lignes de gaz périphériques au réacteur, le risque d'explosion ne peut être négligé. En fonctionnement normal, la pression maximale du réacteur est régulée par un déverseur qui évacue le trop-plein de pression vers le conduit d'évacuation des gaz. Lors des expériences, la pression est mesurée en continu dans le réacteur et à différents endroits des lignes de gaz. En cas de dépassement des valeurs limites de sécurité prescrites par l'opérateur, le système informatique coupe automatiquement l'arrivée de gaz au réacteur. Pour diminuer encore le risque lié à une défaillance informatique ou mécanique, diverses précautions ont été prises :

- Manomètres placés sur le réacteur et sur le saturateur de gaz visibles à travers le hublot depuis l'extérieur du local ventilé.
- Disque de rupture sur le réacteur calibré à 200 bars, dirigé vers le mur en cas de fuite

- Soupape de sécurité calibrée à 2.5 bars sur la ligne gaz en aval du réacteur pour protéger l'analyseur FTIR. La sortie est redirigée vers un conduit d'aération en cas de dépassement de la pression maximale admissible au FTIR.
- Soupape de sécurité calibrée à 40 bars sur le saturateur de gaz et dont la sortie est dirigée vers le mur.

8.1.7 Le stockage des produits chimiques ou biologiques

La commande des produits chimiques se fait par l'intermédiaire du magasin de produits chimiques de l'ULg. Les produits une fois arrivés sont stockés dans un endroit approprié pour éviter toute dégradation de leur qualité. Le stockage et le transport des produits chimiques se font en conservant l'emballage original de transport.

Selon les cas, le stockage se fait dans un frigo à proximité de l'installation ou dans une pièce ventilée prévue à cet effet en dehors de la halle de chimie appliquée. La présence de produits chimiques en dehors des lieux de stockage est limitée au strict nécessaire. La pièce ventilée prévue pour le stockage des produits chimiques ne disposant pas d'un système d'aération performant, il convient de patienter une à deux minutes entre l'ouverture de la porte de cette pièce et l'entrée dans la pièce.

Les produits chimiques concernés ne présentent pas de risques particuliers lors de leur stockage. Ils sont stockés par famille de risques. Leurs fiches de sécurité se trouvent dans la farde de l'installation. Il n'y a pas manipulation de produits biologiques.

8.1.8 Le matériel de travail, les outils, les machines

Les surfaces de travail sont en bois traité de type « paillasse de laboratoire» et ne présentent pas de risque de réaction avec les produits manipulés. Les outils de travail sont rangés dans l'atelier des techniciens dans la halle de chimie appliquée. Leur état est régulièrement contrôlé et les travailleurs sont suffisamment formés à leur utilisation.

8.1.9 Les commandes et signaux

Le panneau de contrôle de l'installation se situe juste à l'extérieur du local ventilé où se trouve le réacteur de dégradation. L'ordinateur permet l'acquisition de données ainsi que le contrôle des lignes de gaz. Un boitier de contrôle fourni avec le réacteur permet l'acquisition de données ainsi que le contrôle du réacteur. Le panneau de contrôle peut être relié à internet de sorte que les données lues en direct puissent être consultables par un accès sécurisé depuis n'importe quel ordinateur connecté à internet.

En cas de fonctionnement de l'installation en dehors des limites de sécurité prescrites par l'opérateur, le système informatique coupe automatiquement l'alimentation en gaz du réacteur. Le système de chauffe du réacteur est coupé automatiquement en cas de dépassement des valeurs consignes de température et de pression au sein du réacteur.

8.1.10 Les positions de travail

L'installation étant prévue pour pouvoir fonctionner automatiquement, les principales manipulations manuelles auront lieu entre les expériences. Lors du remplissage de l'humidificateur de gaz au moyen d'eau distillée, il conviendra d'utiliser systématiquement un entonnoir pour éviter de renverser de l'eau à proximité de l'installation et des fils électriques environnants. Le réservoir de l'humidificateur sera toujours entièrement vidé avant

remplissage et le volume de remplissage sera toujours le même afin d'éviter tout débordement d'eau. La fréquence de remplissage ne dépassera pas une fois tous les trois mois.

8.1.11 Les efforts et les manutentions

Pas d'effort ni de manutention spécifiques.

8.1.12 L'éclairage

L'éclairage du local ventilé se fait par lumière naturelle au travers d'une plaque de plastique translucide au plafond du local. Un tube lumineux est également prévu, son interrupteur se trouve en dehors du local ventilé, au dessus de l'interrupteur pour l'aération. En dehors du local ventilé, l'éclairage de la halle est suffisant pour le poste de contrôle.

En cas de coupure brusque de courant, un éclairage de secours situé à proximité de l'installation prend le relais et éclaire le chemin vers la sortie. L'état de charge de cet éclairage secondaire fonctionnant sur batterie est contrôlé régulièrement. De plus, une lampe de poche se trouve dans l'atelier des techniciens dans un endroit facilement accessible dans le noir.

8.1.13 Le bruit

Les principaux bruits sont ceux de la ventilation du local et de l'agitateur du réacteur. Ils sont largement en-dessous des limites autorisées. En cas d'arrêt d'urgence de l'installation, les vannes pneumatiques relâchent brusquement de l'air comprimé, laissant entendre un bruit semblable à une détonation d'arme à feu. Afin d'éviter cela, des silencieux d'échappement ont été rajoutés.

8.1.14 Les ambiances thermiques

La température est celle de la Halle de Chimie Appliquée. Un système de chauffage est prévu pour l'hiver mais ne fonctionne qu'en mode anti-gel en dehors des heures d'ouverture de la Halle. Il n'y a pas de climatisation en été, mais si nécessaire, les portes de la halle sont maintenues ouvertes pour permettre une circulation supplémentaire d'air. Aucun problème lié à l'humidité n'a été constaté.

8.1.15 Les risques d'exposition aux radiations

Les radiations infrarouges émises par l'analyseur FTIR sont confinées et l'analyseur dispose de tous les équipements de sécurité nécessaires pour empêcher les radiations en dehors de la cellule d'analyse. Aucune autre source de radiation dangereuse ne se trouve à proximité.

8.1.16 Les risques chimiques

La liste des produits chimiques utilisés ainsi que les fiches de sécurité associées sont disponibles dans la farde de l'installation, à proximité immédiate du panneau de contrôle de celle-ci.

La manipulation de produits chimiques et la préparation de solutions se fait principalement dans les laboratoires attenants à la halle de chimie appliquée, ainsi que dans le local ventilé pour ce qui concerne la préparation des échantillons pour l'analyse HPLC. Les équipements de travail adéquats sont disponibles dans ces laboratoires. Les produits utilisés sont bien étiquetés et les procédures de préparation des produits chimiques (principalement la

préparation d'amines à étudier et d'éluant pour les analyses chromatographiques) sont clairement établies.

Les manipulations de produits chimiques se font en local fermé, sous hotte dans les laboratoires (figure 14), ou en local ventilé quand il s'agit du local où se trouve le réacteur de dégradation. La ventilation mise en place dans ce local fonctionne par aspiration et envoie l'air aspiré directement à l'atmosphère. Cette aération a été testée à plusieurs reprises de manière concluante.

Les équipements de protection individuels sont systématiquement portés (gants et lunettes de protection, blouse de laboratoire). Ces équipements de protection individuelle sont disponibles à proximité de l'installation (voir point 3).

Les déchets chimiques sont triés selon les normes en vigueur à l'ULg, dans des bidons prévus exclusivement à cet effet et clairement annotés (figure 15). Une fois remplis, ils sont déposés sur les lieux de collecte spécifique en échange de récipients neufs.

Fig. 14 : Hotte de laboratoire

Fig. 15 : bidons pour les déchets

8.1.17 Les risques biologiques (bactéries, virus, liquides corporels…)

Aucun produit biologique n'est utilisé.

8.1.18 Le contenu du travail

Les procédures de travail sont clairement décrites dans la farde accompagnant l'installation. Ne sont autorisés à travailler sur l'installation de dégradation que l'opérateur principal ou les opérateurs ayant reçu une formation spécifique.

8.1.19 L'organisation du travail

L'organisation du travail se fait selon les normes en vigueur à l'ULg.

8.1.20 Les contraintes de temps

L'installation est prévue pour fonctionner en continu, en ce compris les nuits et les week-ends. Concernant le programme de travail, celui-ci est déterminé d'un commun accord entre l'ULg et Laborelec. Ce programme est régulièrement discuté et mis à jour en fonction des résultats intermédiaires.

8.1.21 Les relations de travail au sein du personnel et avec la hiérarchie

Les décisions se prennent collégialement.

8.1.22 L'environnement psychosocial

Les conditions de vie et d'environnement psychosocial sont en accord avec les normes en vigueur à l'ULg.

Fig. 16 : installation de dégradation des solvants CCS

Analyse lue et approuvée en janvier 2011 par

Pr. G. Heyen, Promoteur de thèse
M. F. Blandina, Laborelec
M. F. Fyon, Technicien Ulg
Mme. A. Grogna, Conseillère en prévention Ulg
M. G. Léonard, Doctorant

8.2 Operating procedures for the degradation test rig (in French)

This section presents in French the operating procedures for the degradation test rig.

La présente section reprend en français les procédures nécessaires au démarrage d'une nouvelle expérience de dégradation des solvants. Il convient bien entendu avant tout début de nouvelle expérience d'établir les conditions expérimentales de la nouvelle expérience en accord avec le planning et les conclusions des tests précédents.

8.2.1 Préparation du circuit de gaz

- Démarrer la ventilation du local ventilé.
- Vérification périodique et remplissage (tous les deux-trois mois) du niveau d'eau dans le saturateur :
    - Ouvrir lentement les deux vannes reliant le saturateur à la cuve de remplissage pour équilibrer les niveaux d'eau dans les deux cuves.
    - Vérifier à l'aide du manomètre que la pression n'excède pas 2 bars dans les cuves. Dans le cas contraire, ouvrir lentement la vanne de remplissage de la cuve de remplissage pour laisser descendre la pression.
    - Dévisser le bouchon supérieur de la cuve de remplissage à l'aide d'une clé anglaise.
    - Vérifier le niveau d'eau dans la cuve de remplissage en y plongeant un tuyau en polyamide bleu (l'eau adhère à la paroi, indiquant le niveau d'eau atteint dans la cuve).
    - Si nécessaire, remplir la cuve de remplissage avec de l'eau distillée. Remplir par la vanne de remplissage en utilisant un entonnoir adéquat.
    - Volume maximal de remplissage des cuves : 5 litres.
    - Vérifier à nouveau le niveau d'eau dans les cuves et continuer à remplir d'eau distillée jusqu'à atteindre le niveau désiré (environs 5cm en dessous du niveau de remplissage maximal).
    - Refermer la vanne de remplissage et revisser le bouchon de la cuve de remplissage.
    - Refermer les deux vannes reliant le saturateur à la cuve de remplissage.

- Vérification de la position de la vanne 3-voies de By-pass du réacteur (elle doit être dans la position Arrivée gaz -> saturateur).
- Vérification de la position de la vanne de sortie du saturateur (elle doit être en position ouverte).
- Vérification de la position de la vanne 3-voies à la sortie gaz après le déverseur (la mettre dans la position désirée : sortie vers l'atmosphère ou vers le FTIR).
- Contrôle des pressions dans bouteilles. Si nécessaire, remplacement des bouteilles en respectant la procédure décrite dans le mode d'emploi fourni avec les centrales de détentes.
- Ouverture des vannes sur les bouteilles de gaz nécessaires pour l'expérience.
- Ouverture des vannes reliant les bouteilles aux centrales de détente.
- Ouverture des vannes reliant les centrales de détente aux conduites de gaz.
- Ajustement si nécessaire des détendeurs pour atteindre une pression de 25 bars dans les conduites (lire la valeur sur le manomètre de la centrale de détente).
- Fermer la vanne d'arrivée des gaz au réacteur pour permettre la mise sous pression du saturateur sur le temps de la préparation de la solution d'amine.

8.2.2 Démarrage de l'acquisition de données et du contrôle de l'installation

- Allumer l'ordinateur.
- Allumer le contrôleur du réacteur 4848.
- Lancer le logiciel Parr.com
- Enregistrer sous (nom de fichier à introduire).
- Démarrer l'acquisition de données pour le réacteur (Température, vitesse de rotation et pression), à la fréquence d'une acquisition toutes les 60 secondes.
- Lancer le logiciel Labview.
- Encoder le nom de fichier d'enregistrement, les valeurs désirées de débit des gaz (en fonction de l'expérience), la température souhaitée pour le ruban chauffant (généralement 35°C), la température souhaitée pour le saturateur et la cuve de remplissage (généralement 25°C, en fonction de la température ambiante), la fréquence de mesure (une mesure toutes les 60 secondes), les pressions minimale et maximale souhaitées au saturateur (qui serviront de régulation pour la pression du réacteur) et actionner les électrovannes.
- Sauvegarder ces valeurs comme valeurs par défaut.
- Si nécessaire, ajuster les gammes de fonctionnement des débitmètres au moyen d'un câble en T (alimentation 15VDC et RS-232) reliant le débitmètre au PC. Pour ce faire
    - Lancer le logiciel Flowbus DDE et ouvrir la communication avec le débitmètre.
    - Lancer le logiciel Flowview. Sous l'onglets « détails », sélectionner la gamme de débit souhaitée dans le menu déroulant.
    - Actualiser l'échelle de débit dans le programme Labview (à actualiser dans le VI DAQ Assistant ainsi que dans le VI « consignes débitmètres et relais statique ». Dans ce dernier VI, actualiser également les limites des valeurs de consignes admissibles)
- Démarrer l'acquisition de données et le contrôle.
- Amener la pression dans le saturateur à la valeur désirée pour l'expérience (automatique si la valeur de pression désirée a été entrée dans le programme Labview).
- Démarrer le logiciel WinVNC qui permet le contrôle à distance du PC.

8.2.3 Préparation des réactifs

- Le cas décrit est celui de 350 g de MEA 30%. Si nécessaire, ajuster les quantités en suivant la même procédure.
- Pesée sous hotte de la 105,0 g de MEA pure. L'amine est versée dans un becher de 500 ml propre et sec.
- Ajout de 245,0 g d'eau distillée.
- Agitation sous hotte au moyen d'un agitateur magnétique propre et sec.
- Pesée de 300,0 g de la solution obtenue dans le réacteur propre et sec (toujours sous hotte).
- Les 50 g restants sont versés dans un tube d'échantillonnage clairement annoté et sont placés au frigo où ils seront conservés pour analyse.

8.2.4 Mise en route de l'expérience

- Fixer le réacteur à la tête du réacteur dans le local ventilé. Il faut pour cela serrer les 6 boulons de la pièce de fixation, en évitant de serrer deux boulons attenants l'un après

l'autre (pour éviter d'écraser le joint de téflon d'un seul côté). Placer le cylindre métallique de fixation maintenant les deux pièces de serrage du réacteur.

- Ouvrir la vanne d'arrivée des gaz au réacteur afin de procéder à la charge de l'amine.
- Démarrer l'agitation sur le contrôleur du réacteur 4848 et l'amener à 400 rpm au moyen de la molette réglable.
- Patienter plus ou moins deux heures pour la charge de l'amine en CO_2 (temps à adapter en fonction de la composition en CO_2 de l'alimentation).
- Peser le réacteur après charge. Pour ce faire :
    - Fermer la vanne d'arrivée des gaz au réacteur.
    - Enlever le cylindre de fixation de la tête du réacteur.
    - Desserrer les boulons qui maintiennent le réacteur.
    - Peser le réacteur et noter la valeur.
    - Replacer le réacteur sur sa tête et le fixer comme décrit précédemment.
- Démarrer la circulation d'eau au bain thermostatisant pour le condenseur. Vérifier que le niveau d'eau dans le bain thermostatisant est suffisant, et si nécessaire, le remplir au moyen d'eau distillée.
- Ouvrir la vanne de sortie des gaz du réacteur après deux heures, ou dès que la charge en CO_2 est terminée (c'est le cas lorsque la température n'augmente plus et qu'on observe une cassure dans l'évolution de la pression).
- Régler manuellement le déverseur afin que la pression dans le réacteur se stabilise à la pression désirée.
- Prendre un échantillon de la solution après charge. Pour ce faire :
    - Fermer la vanne d'arrivée des gaz au réacteur.
    - Ouvrir lentement la vanne de prise d'échantillon, en disposant un tube eppendorf pour récolter l'échantillon.
    - Prélever d'abord une volume de 1,5ml afin de nettoyer le conduit de prise d'échantillon de son volume mort.
    - Prélever dans un deuxième tube eppendorf un échantillon de 1,5ml, l'annoter clairement et le placer au frigo où il sera conservé pour analyse.
    - Ouvrir la vanne d'arrivée des gaz au réacteur.
- Ouvrir le robinet pour le circuit d'eau de refroidissement de l'agitateur magnétique du réacteur et de la sonde de pression. Ajuster le débit de telle sorte qu'un mince filet d'eau coule en permanence.
- Ouvrir le robinet d'eau du circuit de refroidissement du bain thermostatisant pour le condenseur.
- Placer la coque chauffante de telle sorte que le réacteur soit entièrement dedans. Point capital car un oubli pourrait causer la surchauffe de la coque et gravement endommager le matériel.
- Encoder les température de consigne et température d'alarme souhaitées pour l'expérience sur le contrôleur 4848 (voir mode d'emploi du contrôleur).
- Démarrer le chauffage au moyen de l'interrupteur sur le contrôleur du réacteur 4848. Deux puissances de chauffe sont disponibles, la première suffit, mais il est possible d'utiliser la deuxième dans un premier temps pour chauffer plus rapidement. Dans ce cas, revenir à la première puissance de chauffe lorsque la température dans le réacteur se situe environs 20° en dessous de la température désirée (cela afin de prévenir un dépassement trop important de la température de consigne).
- Après une semaine, prendre un échantillon de 1,5 ml suivant la procédure de prise d'échantillon décrite ci-dessus.

8.2.5 Fin de l'expérience

- Après deux semaines, prendre un échantillon de 1,5 ml suivant la procédure de prise d'échantillon décrite ci-dessus.
- Couper le chauffage du réacteur.
- Stopper le logiciel d'acquisition de données Parr.
- Stopper le logiciel Labview (ce qui coupera l'alimentation en gaz automatiquement).
- Fermer les vannes sur les bouteilles de gaz nécessaires pour l'expérience.
- Fermer les vannes reliant les bouteilles aux centrales de détente.
- Fermer les vannes reliant les centrales de détente aux conduites de gaz.
- Vider la pression restante en ouvrant lentement (pour éviter l'entraînement de liquide dans le condenseur) le déverseur jusqu'à sa position d'ouverture maximale.
- Une fois le réacteur refroidi et la pression revenue à la pression atmosphérique, couper l'agitation et éteindre le contrôleur du réacteur 4848.
- Fermer les robinets d'eau pour les circuits de refroidissement (réacteur et bain thermostatisant).
- Couper l'alimentation du bain thermostatisant.
- Démonter le réacteur et le peser. Noter la valeur.
- Prélever 50 ml d'échantillon dans un tube d'échantillonnage clairement annoté et le placer au frigo où il sera conservé pour analyse.
- Vider le restant de la solution d'amine dans le bidon prévu à cet effet.

8.2.6 Nettoyage du réacteur : 1ère phase

- Cette procédure vise le nettoyage qui est effectué après chaque expérience, pas le nettoyage du système d'agitation magnétique du réacteur qui doit cependant être effectué tous les 6 mois en suivant la procédure décrite dans le mode d'emploi du réacteur.
- Nettoyer le réacteur en le rinçant plusieurs fois à l'eau distillée et si nécessaire à l'acétone. Sécher à l'air comprimé ou à l'étuve. Si nécessaire, frotter les parois du réacteur avec une éponge (côté vert de l'éponge).
- Répéter l'opération jusqu'à ce que la conductivité de la solution de rinçage descende en dessous de 2 mS/cm.
- Nettoyer de la même façon que le réacteur les éléments plongeants dans le réacteur (si nécessaire, les démonter pour procéder au nettoyage) : Thermocouple, dip tube, cooling coil, bushing en téflon. Vérifier de nouveau la qualité du nettoyage par mesure de conductivité de l'eau de rinçage.
- Nettoyer le conduit d'échantillonnage par passage d'eau distillée, acétone, air comprimé.
- S'assurer le tuyau d'arrivée des gaz reliant le saturateur au réacteur est propre. Si nécessaire, démonter la ligne d'arrivée des gaz jusqu'au clapet anti-retour et la nettoyer (dans l'ordre : eau distillée, acétone, air comprimé).
- Purger les conduites de sortie du gaz par passage d'air comprimé pendant 5 minutes. Pour ce faire, ouvrir la vanne d'arrivée d'air comprimé et orienter la vanne 3-voies située en amont du saturateur de façon à ce que l'air comprimé purge la partie aval des conduites.
- Démonter la portion de conduite située entre le réacteur et le condenseur. Pour ce faire, il est nécessaire de démonter d'abord la paroi extérieure du système d'agitation magnétique du réacteur et ensuite le thermocouple (simple démontage avec clé Allen, tournevis et clé à molette).

- Nettoyer soigneusement cette portion de conduite pour enlever les cristaux qui s'y seraient formés (même procédure de nettoyage que pour le réacteur).
- Si nécessaire, démonter le sampling cylinder et le nettoyer en suivant la même procédure que pour le réacteur (eau distillée, acétone, séchage).
- Remonter tous les éléments dans l'ordre contraire de leur démontage (commencer par le sampling cylinder et terminer par les éléments plongeants dans le réacteur).
- Rincer une nouvelle fois tous les éléments à l'eau distillée et contrôler la conductivité de l'eau de rinçage.

8.2.7 Nettoyage du réacteur : 2ème phase

- Suivre la procédure de Préparation du Circuit de Gaz décrite ci-dessus.
- Suivre la procédure de Démarrage de l'Acquisition de Données et du Contrôle de l'Installation décrite ci-dessus. On recommande un nettoyage à l'azote uniquement, à un débit de 200 mln/min. Les pressions minimale et maximale souhaitées au saturateur dans le cas du nettoyage sont respectivement 3,8 et 4,2 bar)
- Remplir le réacteur d'eau distillée (approximativement 400 ml) et mesurer la conductivité de cette eau. La noter.
- Fixer le réacteur à la tête du réacteur dans le local ventilé. Il faut pour cela serrer les 6 boulons de la pièce de fixation, en évitant de serrer deux boulons attenants l'un après l'autre (pour éviter d'écraser le joint de téflon d'un seul côté). Placer le cylindre métallique de fixation maintenant les deux pièces de serrage du réacteur.
- Ouvrir la vanne d'arrivée des gaz au réacteur afin de procéder au barbotage d'azote.
- Démarrer l'agitation sur le contrôleur du réacteur 4848 et l'amener à 400 rpm au moyen de la molette réglable.
- Démarrer la circulation d'eau au bain thermostatisant pour le condenseur. Vérifier que le niveau d'eau dans le bain thermostatisant est suffisant, et si nécessaire, le remplir au moyen d'eau distillée.
- Ouvrir la vanne de sortie des gaz du réacteur après deux heures, ou dès que la charge en CO_2 est terminée (c'est le cas lorsque la température n'augmente plus et qu'on observe une cassure dans l'évolution de la pression).
- Régler manuellement le déverseur afin que la pression dans le réacteur se stabilise à la pression désirée.
- Ouvrir le robinet pour le circuit d'eau de refroidissement de l'agitateur magnétique du réacteur et de la sonde de pression. Ajuster le débit de telle sorte qu'un mince filet d'eau coule en permanence.
- Ouvrir le robinet d'eau du circuit de refroidissement du bain thermostatisant pour le condenseur.
- Placer la coque chauffante de telle sorte que le réacteur soit entièrement dedans. Point capital car un oubli pourrait causer la surchauffe de la coque et gravement endommager le matériel.
- Encoder les température de consigne et température d'alarme souhaitées pour l'expérience sur le contrôleur 4848 (voir mode d'emploi du contrôleur). La température de consigne à encoder est 120°C pour le nettoyage
- Démarrer le chauffage au moyen de l'interrupteur sur le contrôleur du réacteur 4848. Deux puissances de chauffe sont disponibles, la première suffit, mais il est possible d'utiliser la deuxième dans un premier temps pour chauffer plus rapidement. Dans ce cas, revenir à la première puissance de chauffe lorsque la température dans le réacteur se situe environs 20° en dessous de la température désirée (cela afin de prévenir un dépassement trop important de la température de consigne).
- Laisser tourner le nettoyage pendant minimum 12h.

8.2.8 Fin du nettoyage

- Couper le chauffage du réacteur.
- Stopper le logiciel d'acquisition de données Parr.
- Stopper le logiciel Labview (ce qui coupera l'alimentation en gaz automatiquement).
- Fermer les vannes sur les bouteilles de gaz nécessaires pour l'expérience.
- Fermer les vannes reliant les bouteilles aux centrales de détente.
- Fermer les vannes reliant les centrales de détente aux conduites de gaz.
- Vider la pression restante en ouvrant lentement (pour éviter l'entraînement de liquide dans le condenseur) le déverseur jusqu'à sa position d'ouverture maximale.
- Une fois le réacteur refroidi et la pression revenue à la pression atmosphérique, couper l'agitation et éteindre le contrôleur du réacteur 4848.
- Fermer les robinets d'eau pour les circuits de refroidissement (réacteur et bain thermostatisant).
- Couper l'alimentation du bain thermostatisant.
- Démonter le réacteur et mesurer la conductivité de l'eau. Noter la valeur.
- Prélever 50 ml d'échantillon dans un tube d'échantillonnage clairement annoté et le placer au frigo où il sera conservé pour analyse des ions métalliques.
- Vider le restant de la solution d'eau à l'évier.